

Supporting Information

Multivalent Bifunctional Carbosilane Dendrimer Supported Ammonium and Phosphonium Organocatalysts for the Coupling of CO₂ and Epoxides

Lucie Červenková Šťastná,^[†,‡] Alena Krupková,^[†,‡] Roman Petrickovic,^[†,‡] Monika Müllerová,^[†,‡] Jindřich Matoušek,^[‡] Martin Koštejn,^[†] Petra Cuřínová,^[†,‡] Věra Jandová,^[†] Stanislav Šabata,^[†,‡] Tomáš Strašák,^{*[†,‡]}

[†]*Institute of Chemical Process Fundamentals of the Czech Academy of Sciences, v. v. i., Rozvojová 135, 165 02 Prague, Czech Republic*

[‡]*J. E. Purkyně University, České mládeže 8, 40096 Ústí nad Labem, Czech Republic*

Number of pages: 29

Number of figures: 31

Number of tables: 8

Table of Contents

I.	HRMS spectra related to deactivation of the catalyst (Figures S1, S2)	S2
II.	Comparison of catalytic activity with literature (Tables S1, S2)	S3
III.	EDX spectra of nanocomposites (Figures S3 – S5)	S5
IV.	Carbon content in recycled composite catalysts (Figure S6)	S6
V.	NMR spectra (Figures S7 – S30)	S7
VI.	Computational study (Figure S31, Tables S3 – S8)	S19
VII.	References	S27

Figure S1. ESI MS spectrum of Dm_2AOH_8 after 3 catalytic cycles containing AGE oligomers (red and orange). Blue and green colors mark the regions of differently charged dendrimer ions (detail of 4^+ region is shown in Figure S2).

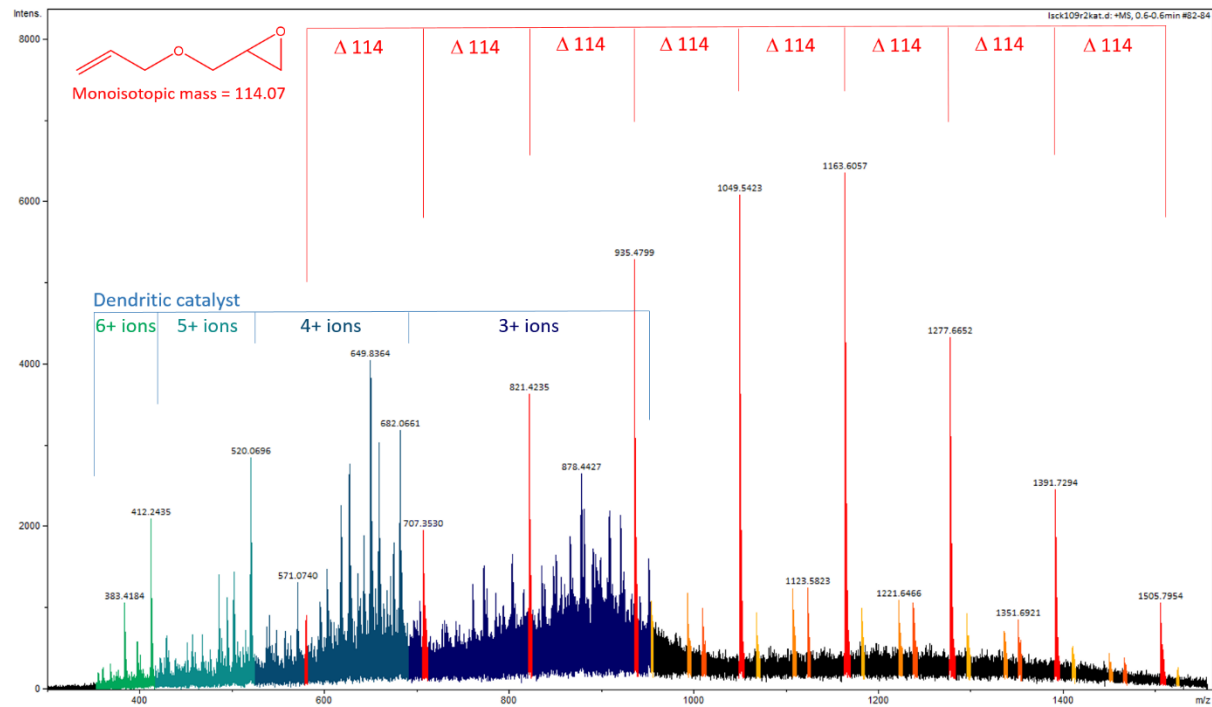


Figure S2. Part of ESI MS spectrum of Dm_2AOH_8 after 3 catalytic cycles showing the region of 4^+ ions (a) in comparison with the same region of the spectrum of original dendrimer (b).

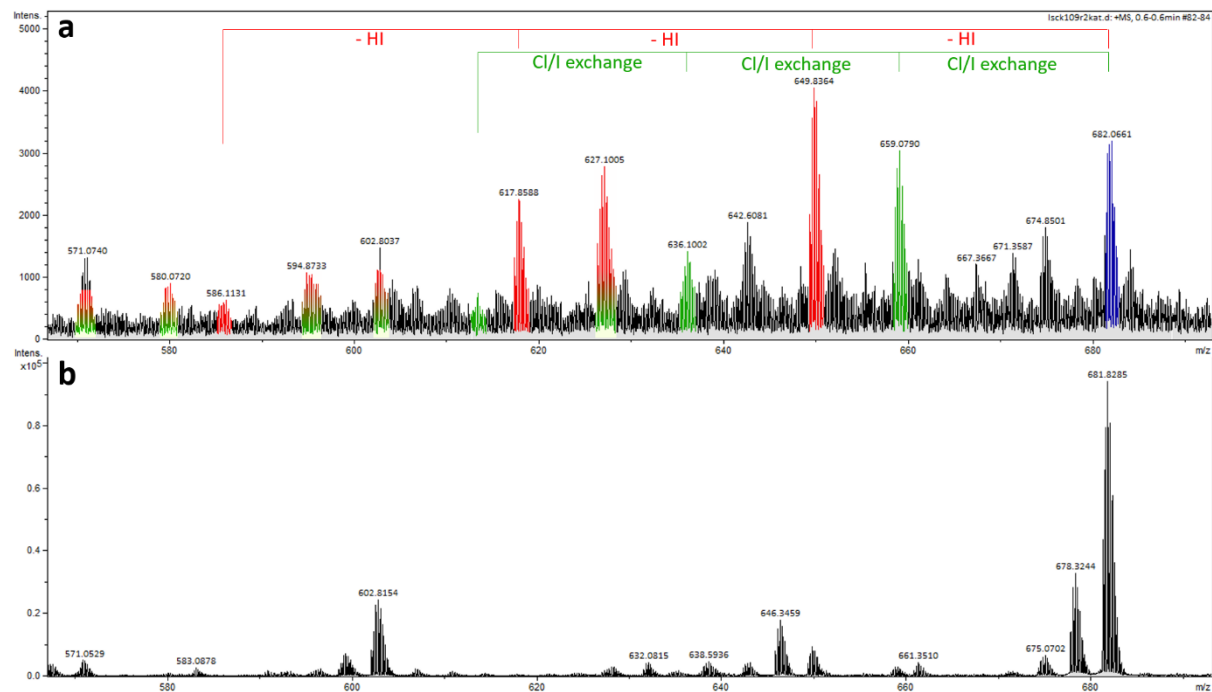


Table S1. Catalytic activity of mono- and bifunctional tetraalkylammonium and phosphonium homogeneous catalysts in cycloaddition of CO₂ to butylene oxide (90°C, 1 MPa, 2 mol % of catalyst, 2 h).

Ammonium catalyst	Yield [%]	Ref.	Phosphonium catalyst	Yield [%]	Ref.
Bu ₄ NCl	33 ^a	1	Bu ₄ PCl	36; 43 ^a	3, 1
Bu ₄ NI	19; 6 ^a	2, 1	Bu ₄ PI	19; 13 ^a	3, 1
HOCH ₂ CH ₂ NBu ₃ Cl	39 ^a	1	HOCH ₂ CH ₂ PBu ₃ Cl	26 ^a	1
HOCH ₂ CH ₂ NBu ₃ I	96; 83 ^a	2, 1	HOCH ₂ CH ₂ PBu ₃ I	92; 82 ^a	3, 1
Dm ₀ AOH ₁	98 ^b	this work	Dm ₀ POH ₁	91 ^b	this work

a) data from graph

b) allyl glycidyl ether as substrate

Table S2. Catalytic activity of selected organocatalysts in cycloaddition of CO₂ to epoxides (selection was made to cover different structural types, top results from each type were included). Entries are ordered first according to the reaction temperature, then according to TOF.

Catalyst structure ^a	Type ^b	Substrate ^c	t [°C]	p [MPa]	Yield [%]	TOF ^d	Ref.
[BMIM]BF ₄	homo	PO	140	2	90	75	4
(PDVB)-HOOC(CH ₂) ₂ ImBr	PIL	PO	140	2	96	55	5
(PDVB)-HO(CH ₂) ₂ ImBr	PIL	PO	140	2	98	55	6
[(nOct-Im-CH ₂) ₂ CHOH]Br ₂	homo	PO	140	1	90	23*	7
N-ethylpyrazolium bromide	homo	AGE	140	2	88	22	8
Me ₂ NCH ₂ COOH.Mel	homo	PO	140	8	98	4.9	9
Dm ₂ AOH ₈	homo	AGE	130	1.5	93	232	this work
Dm ₂ AOH ₈ Mt/KI	supp-2	AGE	130	1.5	99	125	this work
(PS)-HOCH ₂ CH(OH)CH ₂ ImBr	PIL	PO	130	2	97	121	10
H ₂ NEt-guanidinium bromide	homo	PO	130	2.5	95	95	11
HOOCC ₂ CH ₂ PPh ₃ Br	PIL	PO	130	2	83	42	12
nBu-urea-(CH ₂) ₃ -imidazolidinium iodide	homo	PO	130	1.5	97	29	13
HOCH ₂ CH ₂ MelmBr	homo	ECH	125	2	92	174	14
HOCH ₂ CH ₂ NBu ₃	homo	PO	125	2	96	60	14
[EMIM]Br	homo	PO	125	2	83	52	14
Bu ₄ NBr	homo	PO	125	2	74	47	14
choline chloride + urea	homo-2	PO	125	2	71	44	14
[EMIM] ₂ ZnBr ₂ Cl ₂	Zn	PO	120	3.4	98	980*	15
[Bu-Im-CH ₂ C ₆ H ₄ OH]Br	homo	ECH	120	1	90	900	16
[BMIM-CH ₂ OH]Br	homo	PO	120	2	98	98	17
quaternized cellulose	PIL	PO	120	1.2	97	81	18
(PS)-NH(CH ₂) ₆ NMe ₃ I	PIL	AGE	120	1.2	93	39	19
Bu ₄ NI	homo	AGE	120	1.2	71	30	19
H ₂ NCH ₂ COOH.Mel	homo	PO	120	1.2	84	20	20

(chitosan)-ZnCl ₂ + [BMIM]Br	Zn	PO	110	1.5	70	1001*	21
(SiO ₂)-HOOC(CH ₂) ₂ ImBr	supp	PO	110	1.6	99	73	22
(cellulose)-BuImI	PIL	PO	110	1.8	98	40	23
choline chloride + urea	supp-2	PO	110	not given	96	32	24
PEG-guanidinium bromide	homo	PO	110	4	99	25*	25
[BMIM]Br + ZnCl ₂ (6:1)	Zn	PO	100	1.5	98	930*	26
Bu ₄ NBr + Zn(PhSOO) ₂ (46:1)	Zn	PO	100	3	76	152*	27
(HOOC-CH ₂ CH ₂ CH ₂) ₂ ImBr	homo	PO	100	2	99	99	28
Bu ₄ NCl	homo	PO	100	3	72	36	29
Dm ₀ AOH ₁	homo	AGE	90	1	98	24	this work
HOCH ₂ CH ₂ NBu ₃ I	homo	BO	90	1	96	24	2
HOCH ₂ CH ₂ PBu ₃ I	homo	BO	90	1	92	23	3
(PS)-CH ₂ N((CH ₂) ₃ OH) ₃ I	PIL	BO	90	1	93	23	2
Dm ₁ AOH ₄ Mt/KI	supp-2	AGE	90	1	94	16	this work
(SiO ₂)-(CH ₂) ₃ N((CH ₂) ₃ OH) ₃ I	supp	BO	90	1	98	8.2	2
<i>n</i> Bu-urea-(CH ₂) ₃ -imidazolidinium iodide	homo	PO	90	1.5	90	4.3	13
squaramide + Bu ₄ NI	homo-2	HO	80	1	85	85	30
TBD.HBr	homo	PO	80	8	81	4.1	31
(PF)-ImBr	PIL	ECH	80	1	99	4.0*	32
COF + Bu ₄ NCl	supp-2	ECH	80	0.1	72 ^e	1.8 ^e	33
poly(pyridyl imine)	hetero	ECH	80	0.1	72	1.4 ^{f,*}	34
Res-(CH ₂ NH ₂ Bu) ₄ Br ₄	homo	AGE	80	0.5	97	1.3*	35
[Bu-Im-CH ₂ C ₆ H ₄ OH]Br	homo	ECH	70	1	96	32	16
Dm ₃ AOH ₁₆	homo	AGE	70	0.15	84	4.0	this work
[(nOct-Im-CH ₂) ₂ CHOH]Br ₂	homo	PO	70	0.4	99	0.6*	7
HOCH ₂ CH ₂ NBu ₃ I	homo	PO	70	0.4	92	0.6	7
(PMMAG)-dopamine + Bu ₄ NI	supp-2	ECH	60	0.1	100 ^g	4.2*	36
Bu ₄ NI	homo	ECH	60	0.1	36 ^g	1.5	36
(PF)-ImBr	PIL	ECH	60	1	32	1.3*	32
squaramide + Bu ₄ NI	homo-2	HO	45	1	100	2.8	30
Zn-porphyrine-(NBu ₃ Br) ₈	Zn	HO	20	0.1	82	4.3*	37

a) BMIM = 1-butyl-3-methylimidazolium; EMIM = 1-ethyl-3-methylimidazolium; COF = covalent organic framework; PDVB = poly(divinylbenzene); PF = phenol formaldehyde resin; PMMAG = methyl methacrylate copolymer bearing glycidyl groups; PS = polystyrene; Res = resorcin[4]arene; SiO₂ = silica; TBD = 1,5,7-triazabicyclo[4.4.0]dec-5-ene; **b)** hetero = heterogeneous catalyst outside other types; homo = homogeneous catalyst; homo-2 = homogeneous two-component system; PIL = polymeric ionic liquid; supp = homogeneous catalyst immobilized on inorganic support; supp-2 = two-component system, fully or partially immobilized; Zn = Zn²⁺ containing system; **c)** PO = propylene oxide; AGE = allyl glycidyl ether; BO = butylene oxide; ECH = epichlorohydrin; HO = hexene oxide **d)** TOF values are given with respect to amount of nucleophile, recalculated from original data where necessary (complex organocatalysts with more than one nucleophilic center in the molecule, two-component mixtures; recalculated values are marked with asterisk); **e)** data from graph; **f)** TOF per pyridyl imine monomeric unit; **g)** conversion estimated by ¹H NMR without standard

Figure S3. EDX spectrum of nanocomposite Dm₁AOH₄Mt.

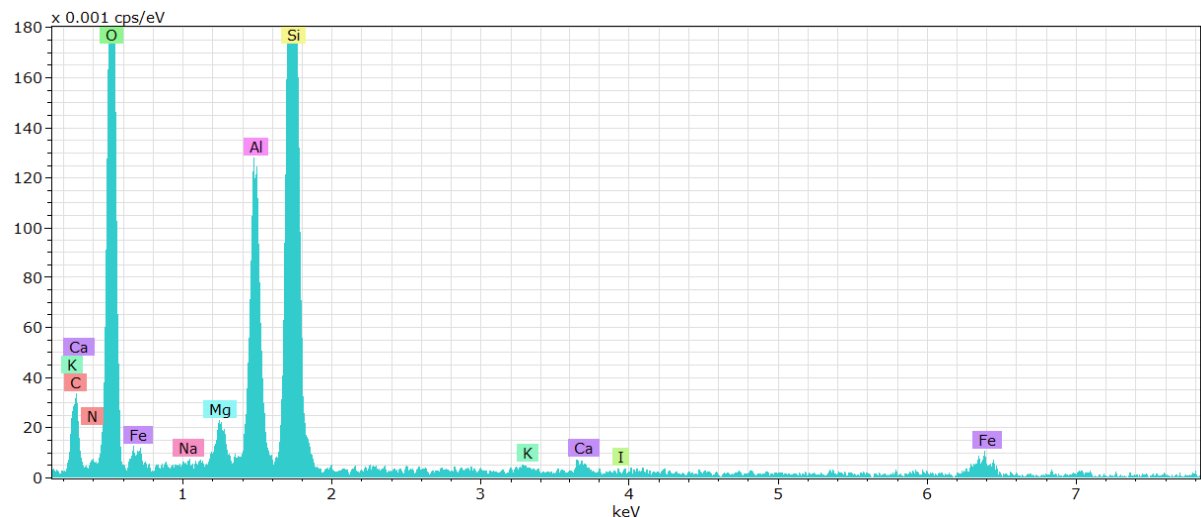


Figure S4. EDX spectrum of nanocomposite Dm₂AOH₈Mt.

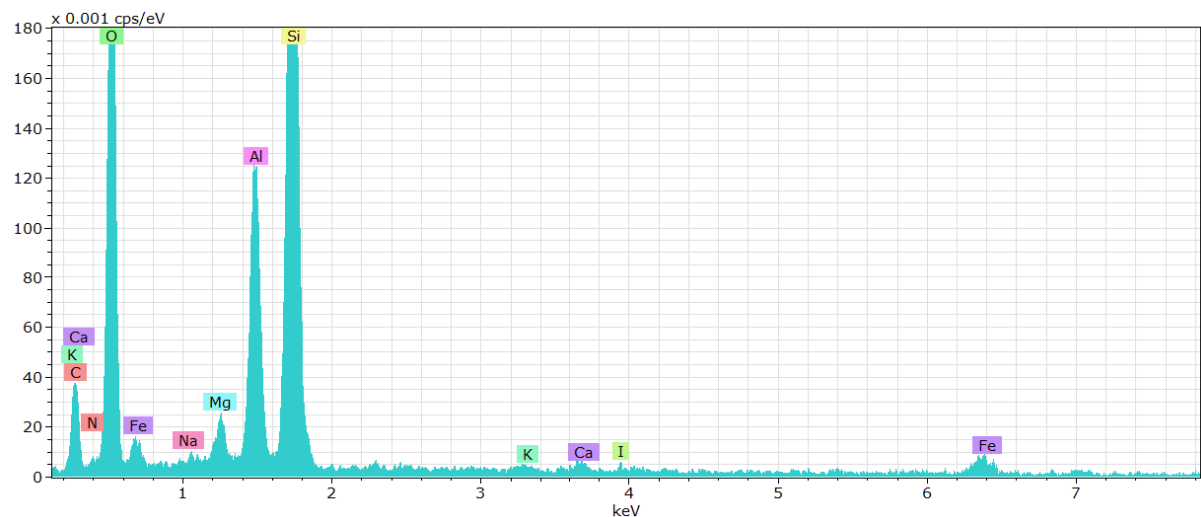


Figure S5. EDX spectrum of nanocomposite Dm₃AOH₁₆Mt.

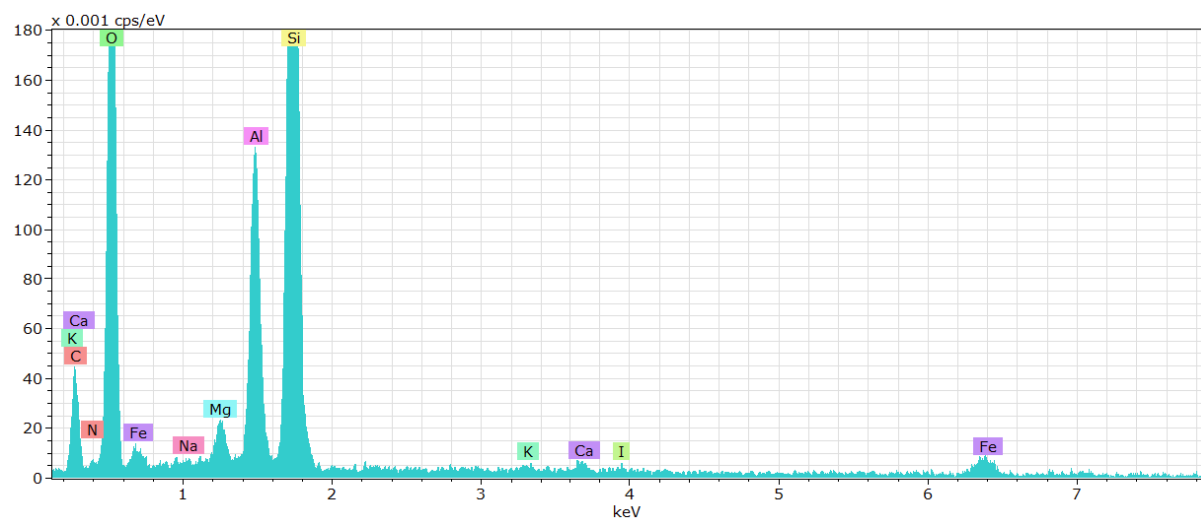


Figure S6. Carbon content in the recycled nanocomposites as a function of number of catalytic cycles as determined by EDX.

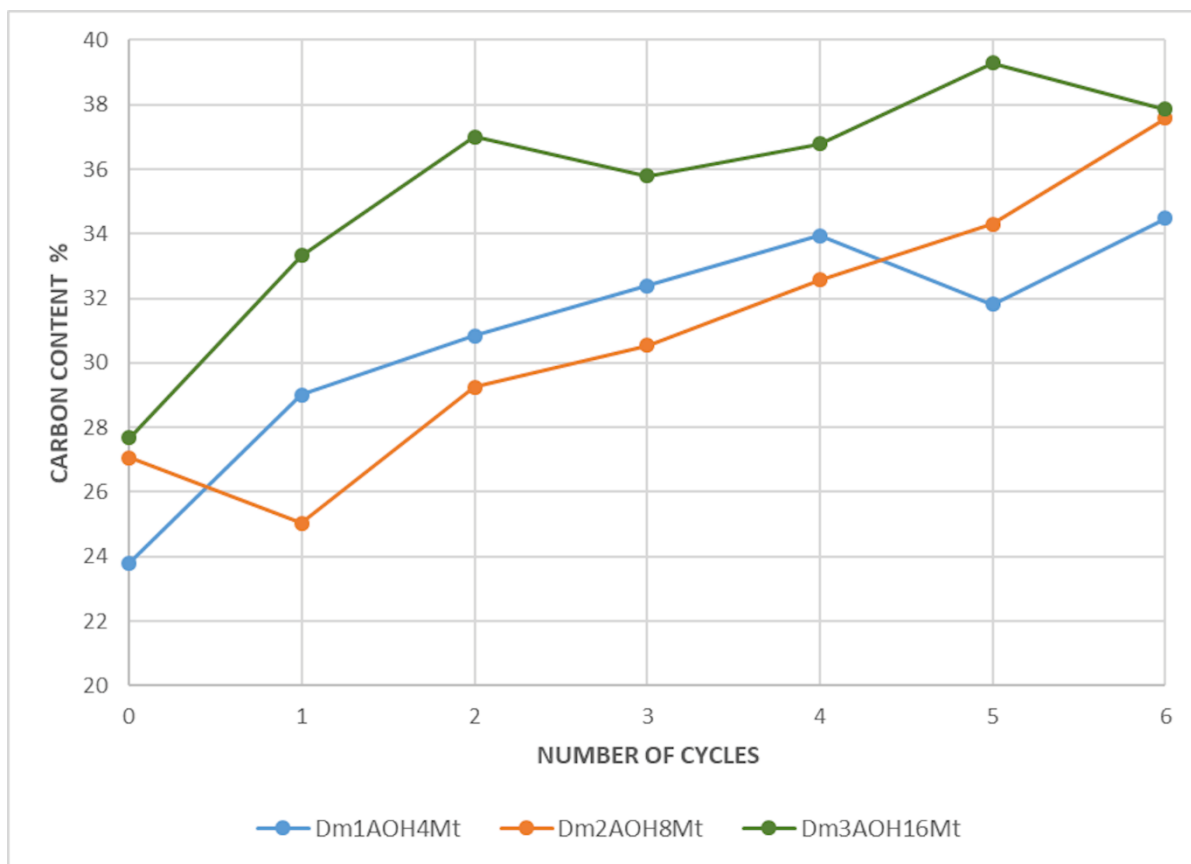


Figure S7. ^1H NMR spectrum of **Dm₀POH₁** in DMSO-d₆.

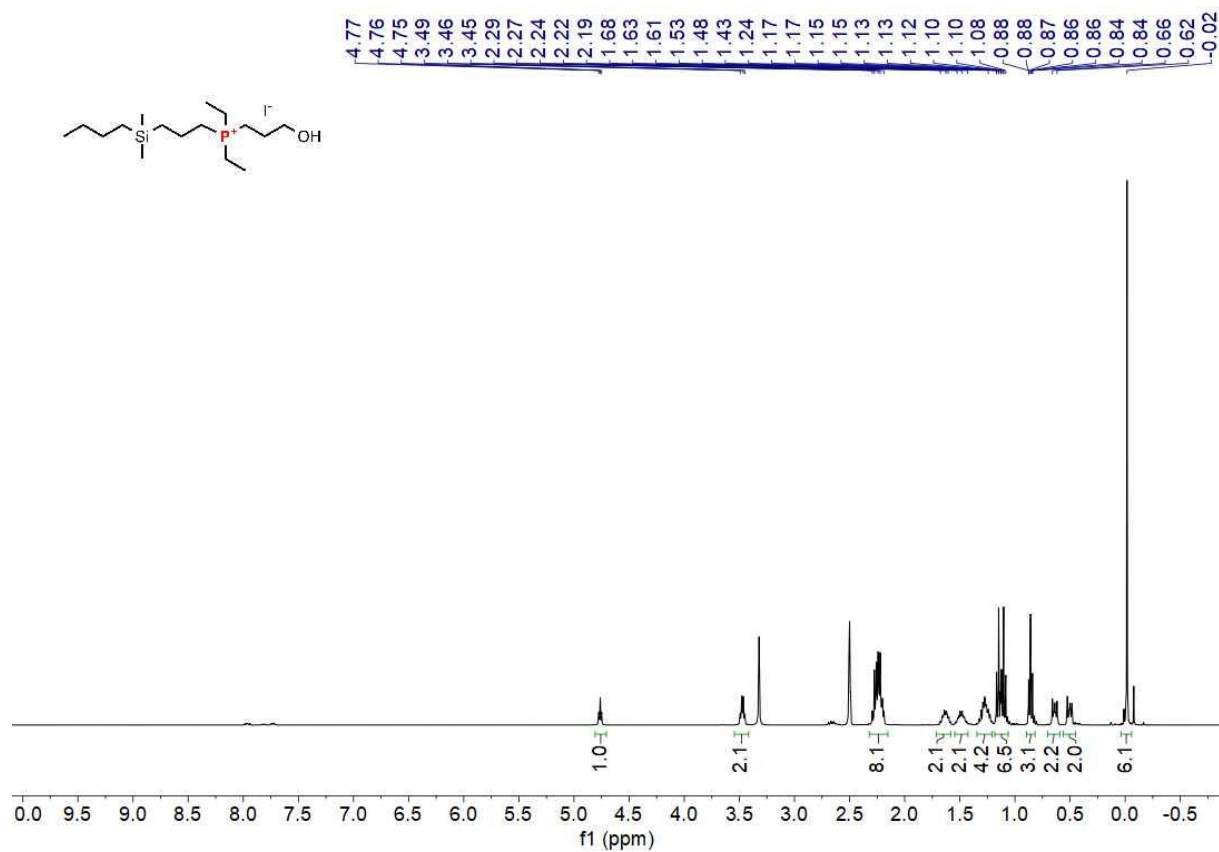


Figure S8. ^{13}C NMR spectrum of **Dm₀POH₁** in DMSO-d₆.

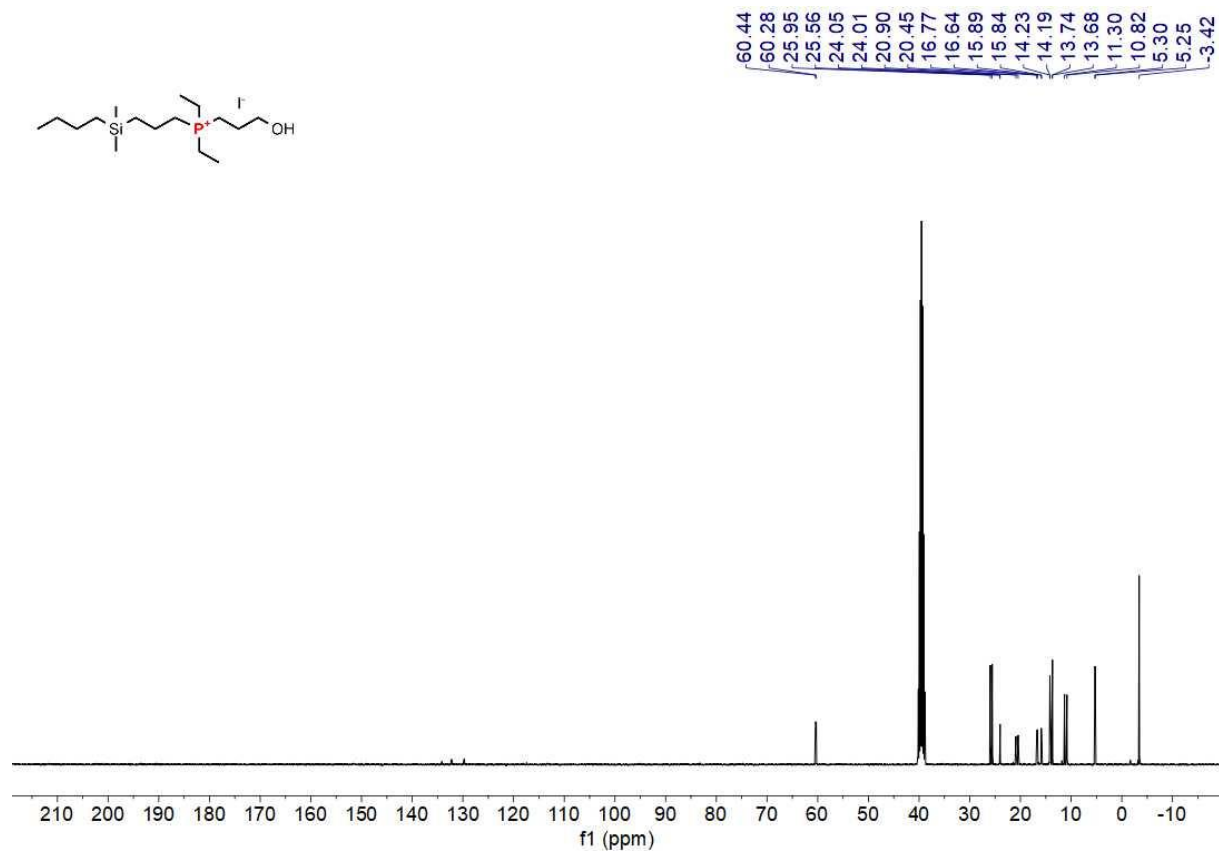


Figure S9. ^{29}Si NMR spectrum of **Dm₀POH₁** in DMSO-d₆.

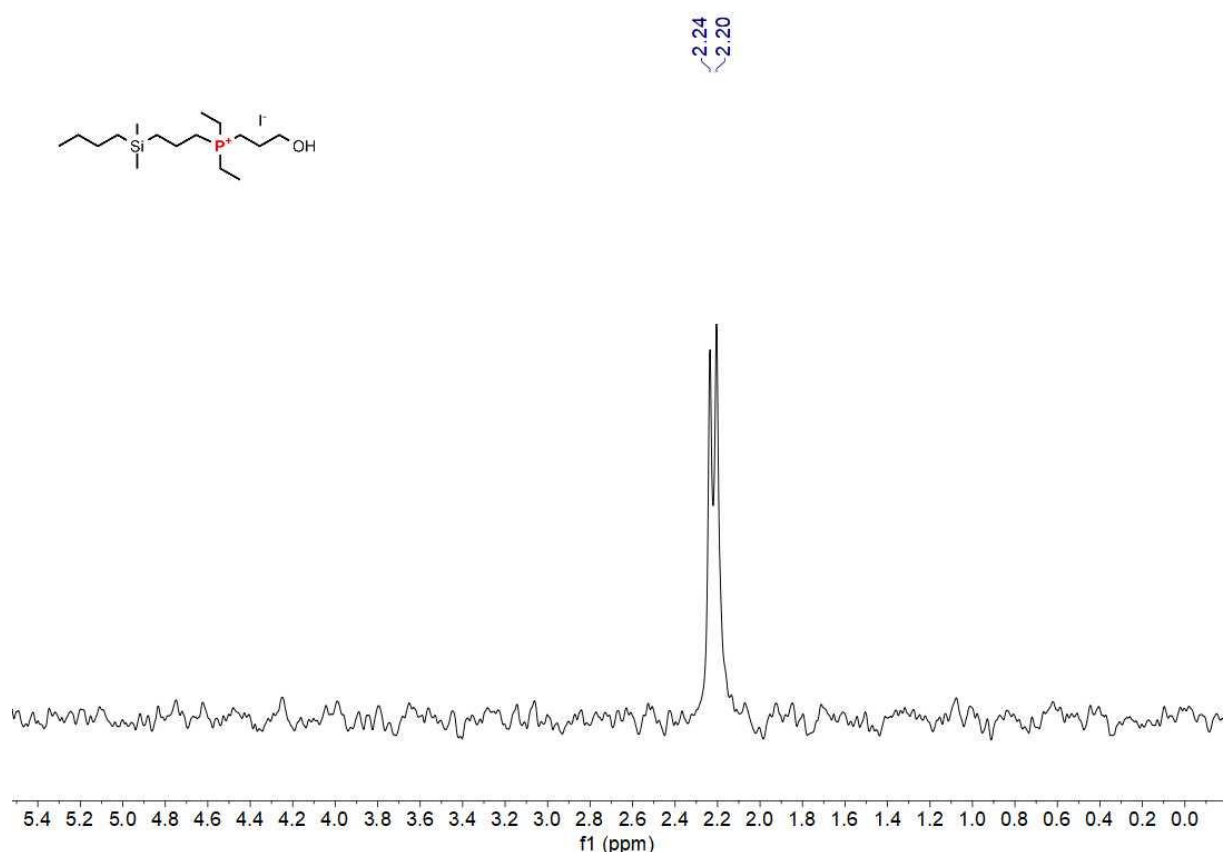


Figure S10. ^{31}P NMR spectrum of **Dm₀POH₁** in DMSO-d₆.

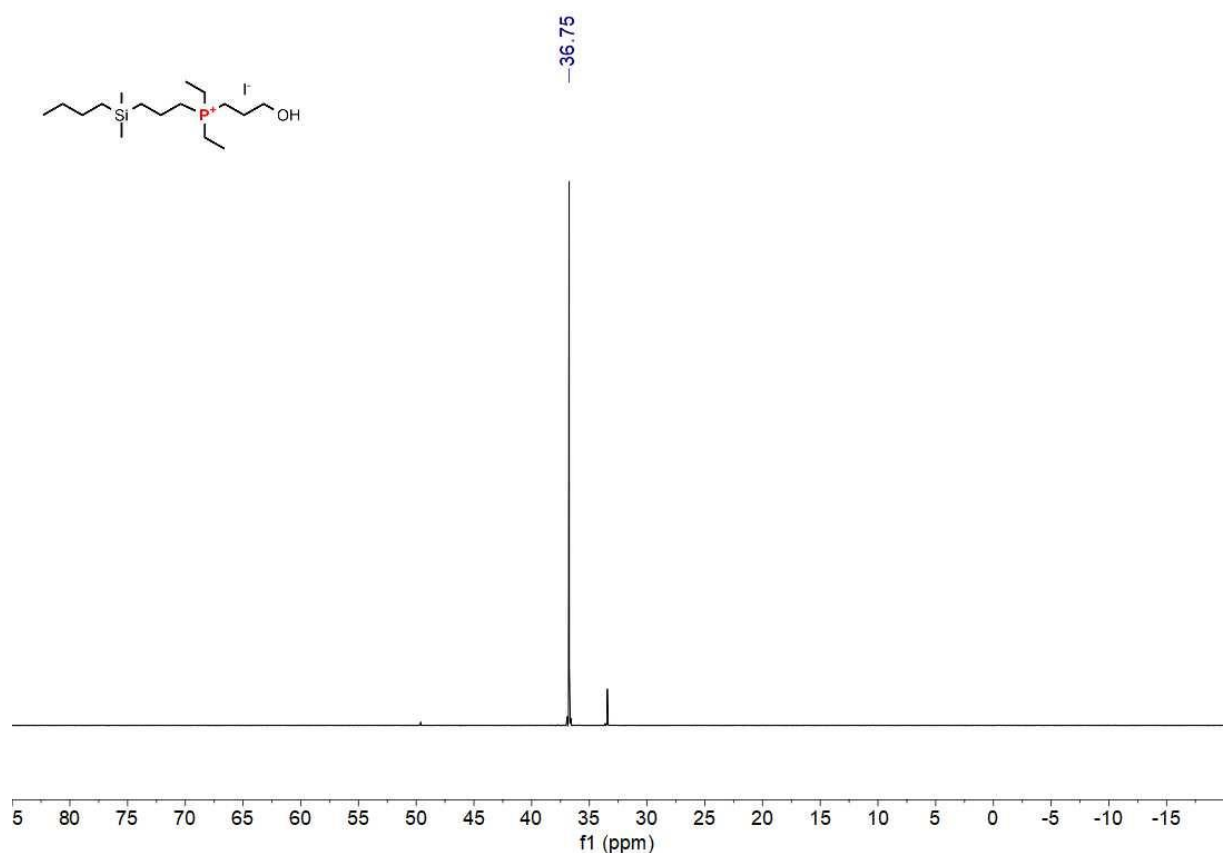


Figure S11. ^1H NMR spectrum of Dm_0AOH_1 in DMSO-d_6 .

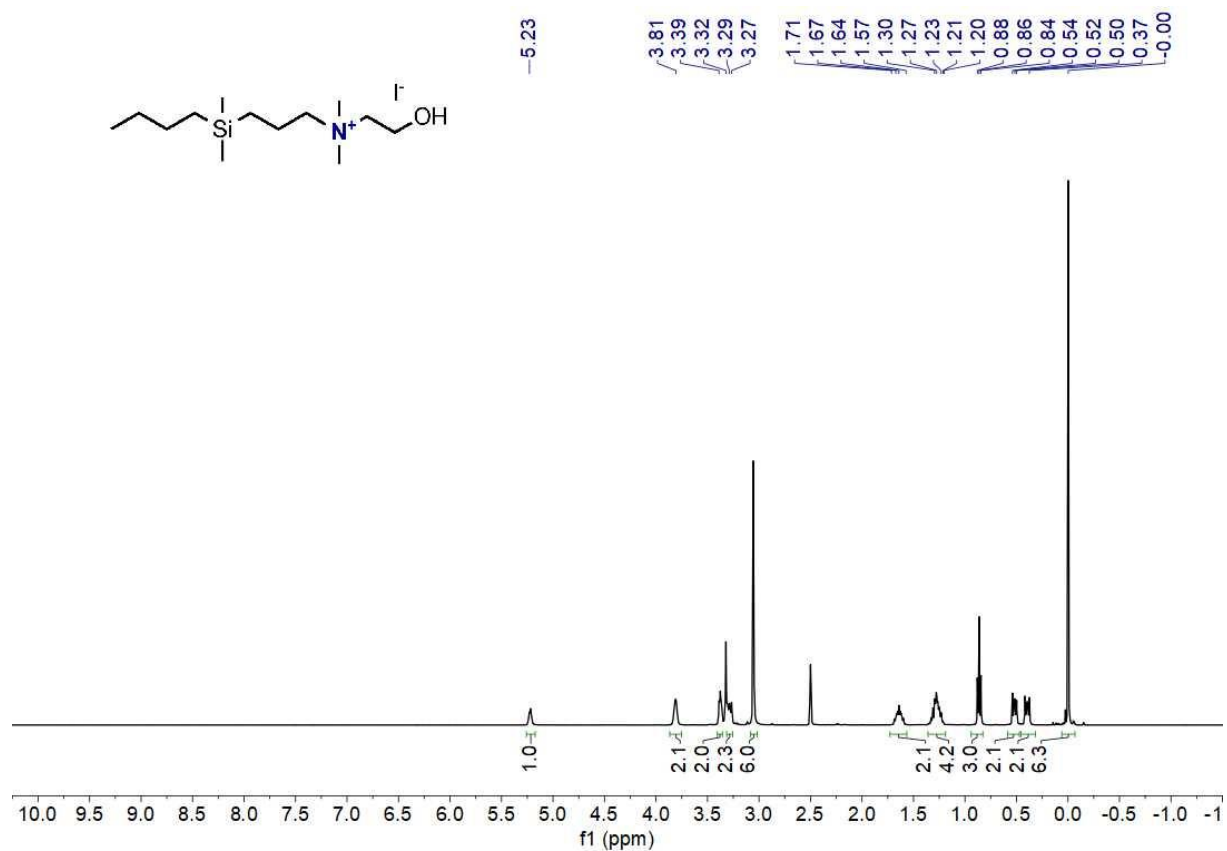


Figure S12. ^{13}C NMR spectrum of Dm_0AOH_1 in DMSO-d_6 .

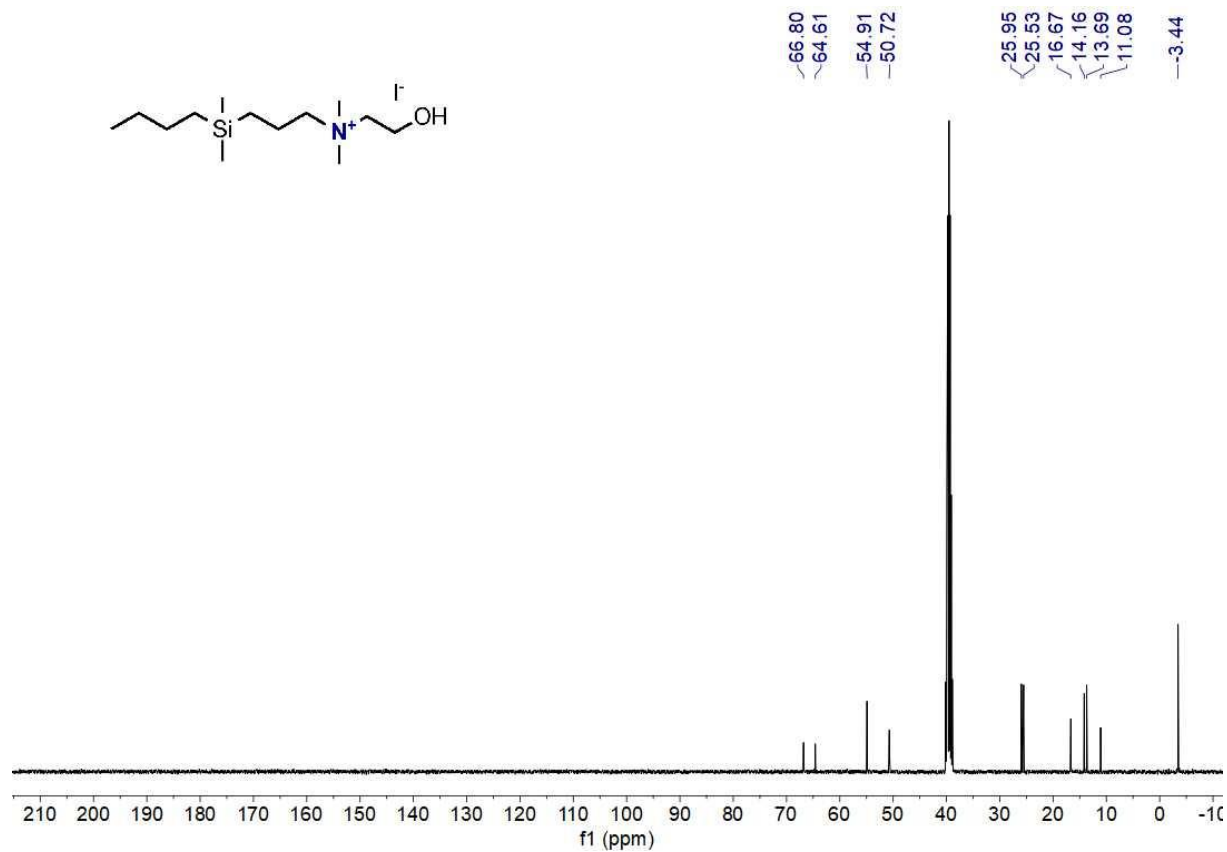


Figure S13. ^{29}Si NMR spectrum of **Dm₀AOH₁** in DMSO-d₆.

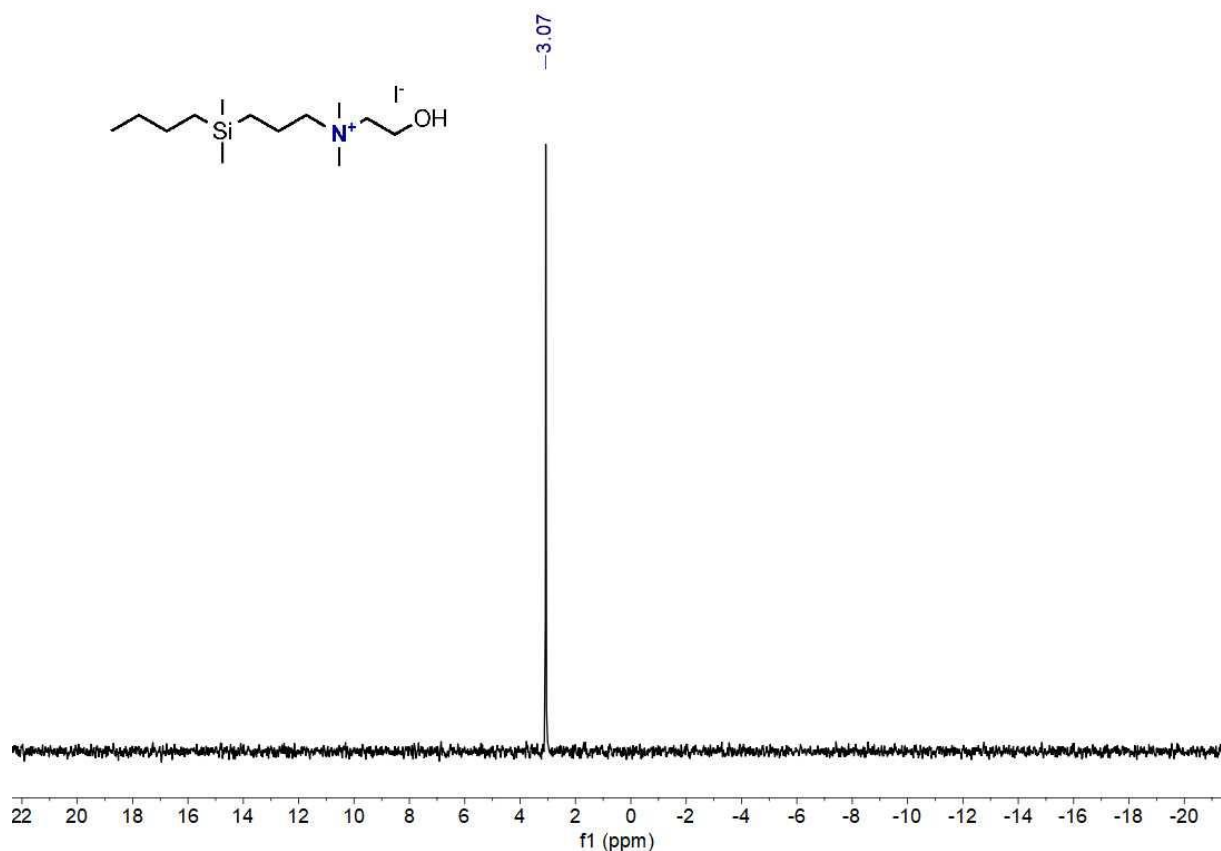


Figure S14. ^1H NMR spectrum of **Dm₁AOH₄** in DMSO-d₆.

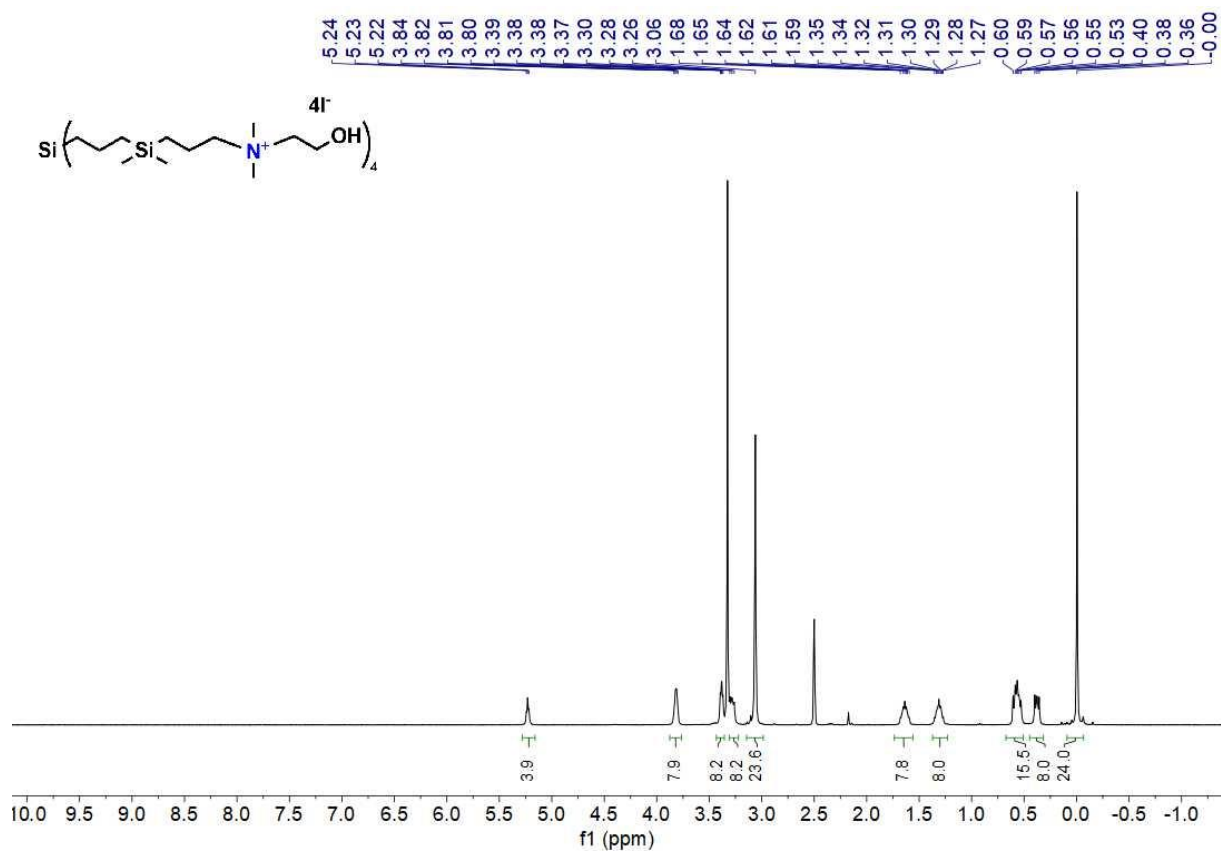


Figure S15. ^{13}C NMR spectrum of Dm_1AOH_4 in DMSO-d_6 .

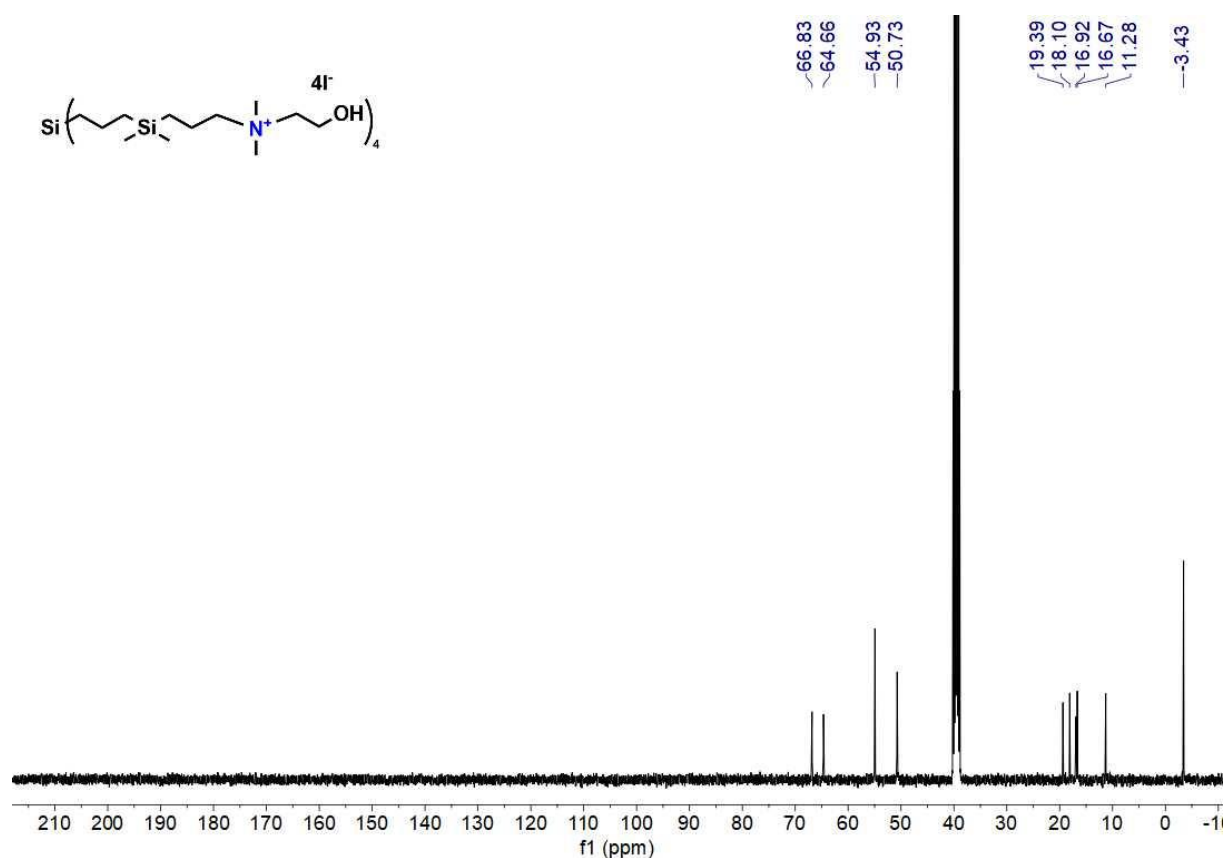


Figure S16. ^{29}Si NMR spectrum of Dm_1AOH_4 in DMSO-d_6 .

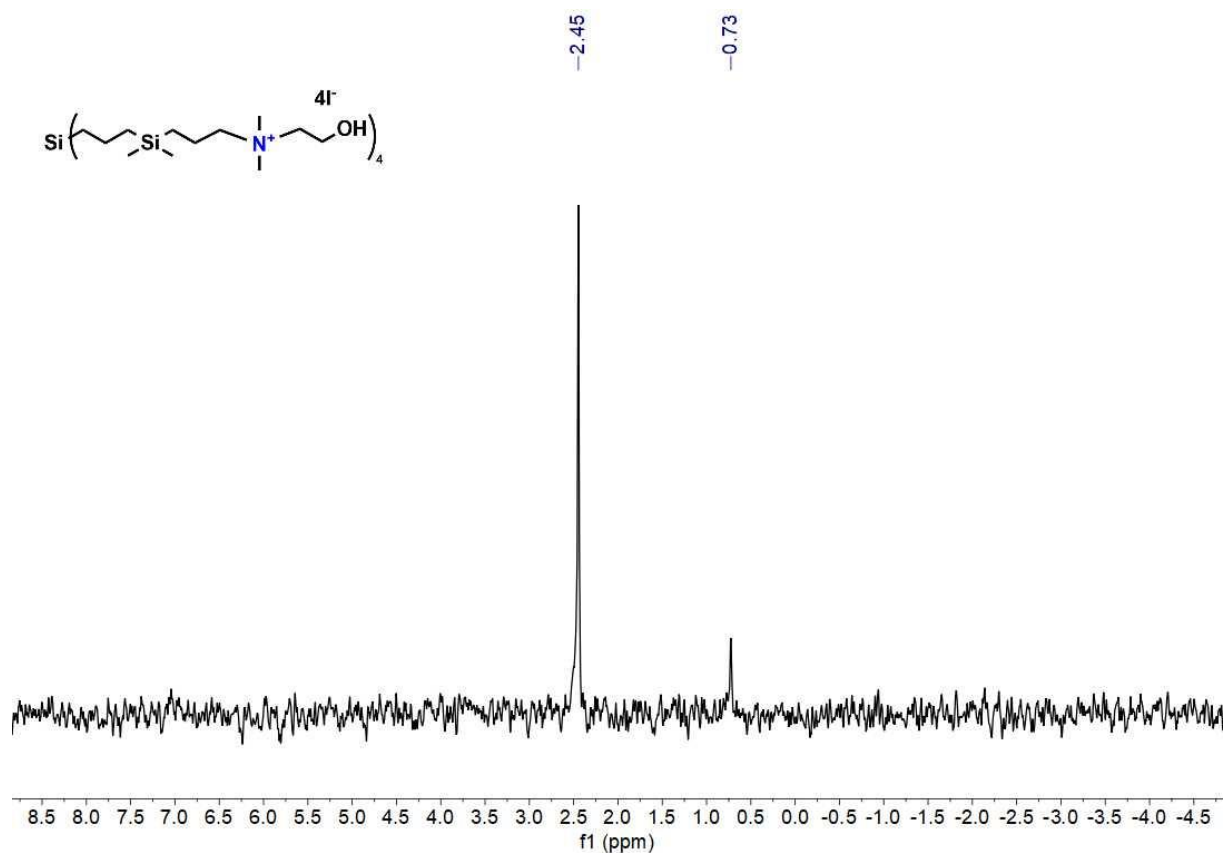


Figure S17. ^1H NMR spectrum of Dm_2AOH_8 in DMSO-d_6 .

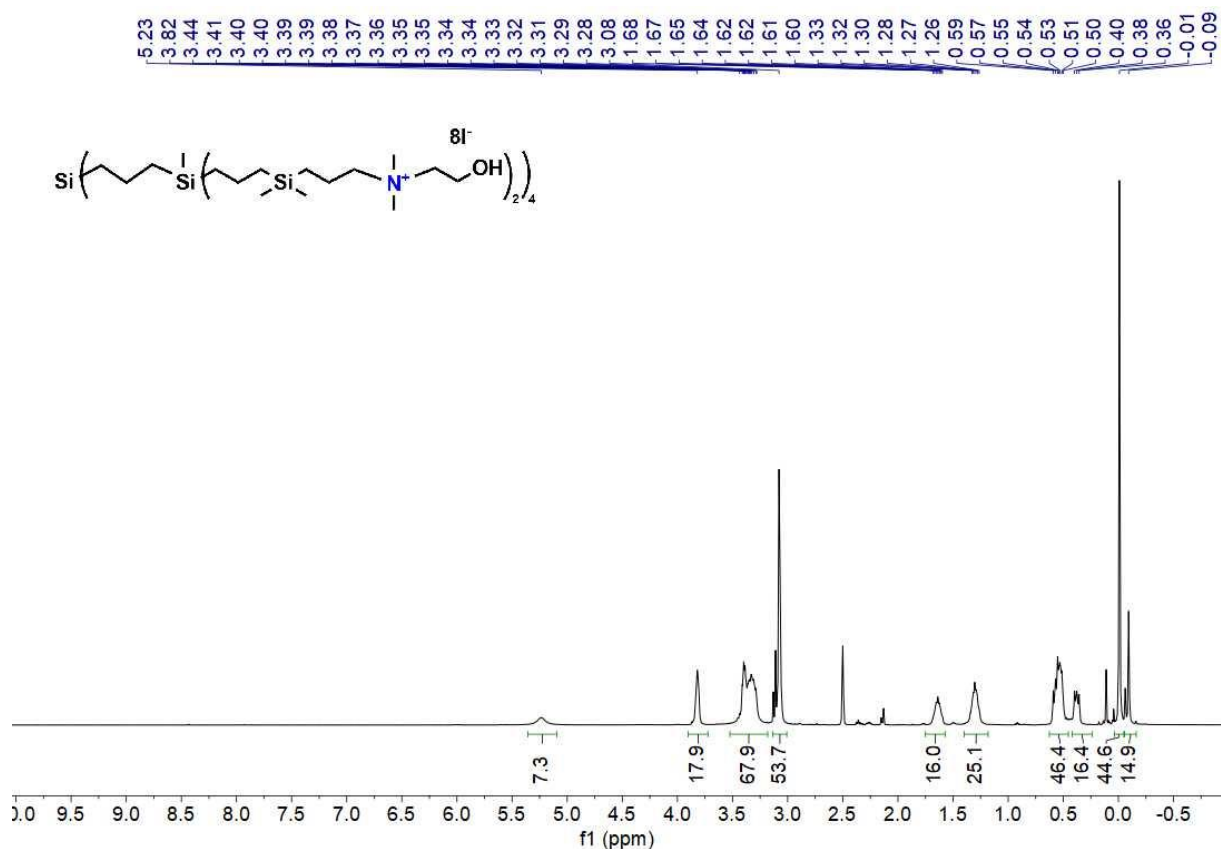


Figure S18. ^{13}C NMR spectrum of Dm_2AOH_8 in DMSO-d_6 .

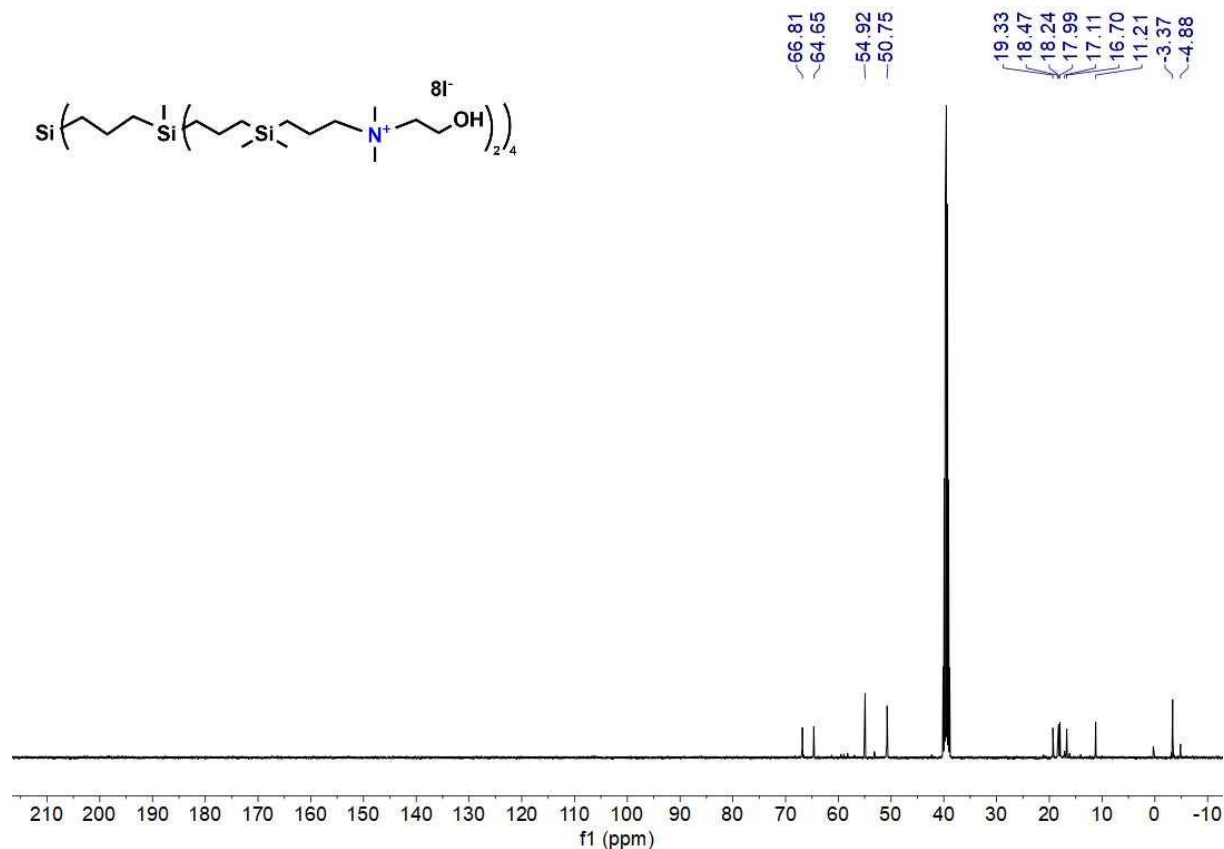


Figure S19. ^{29}Si NMR spectrum of Dm_2AOH_8 in DMSO-d_6 .

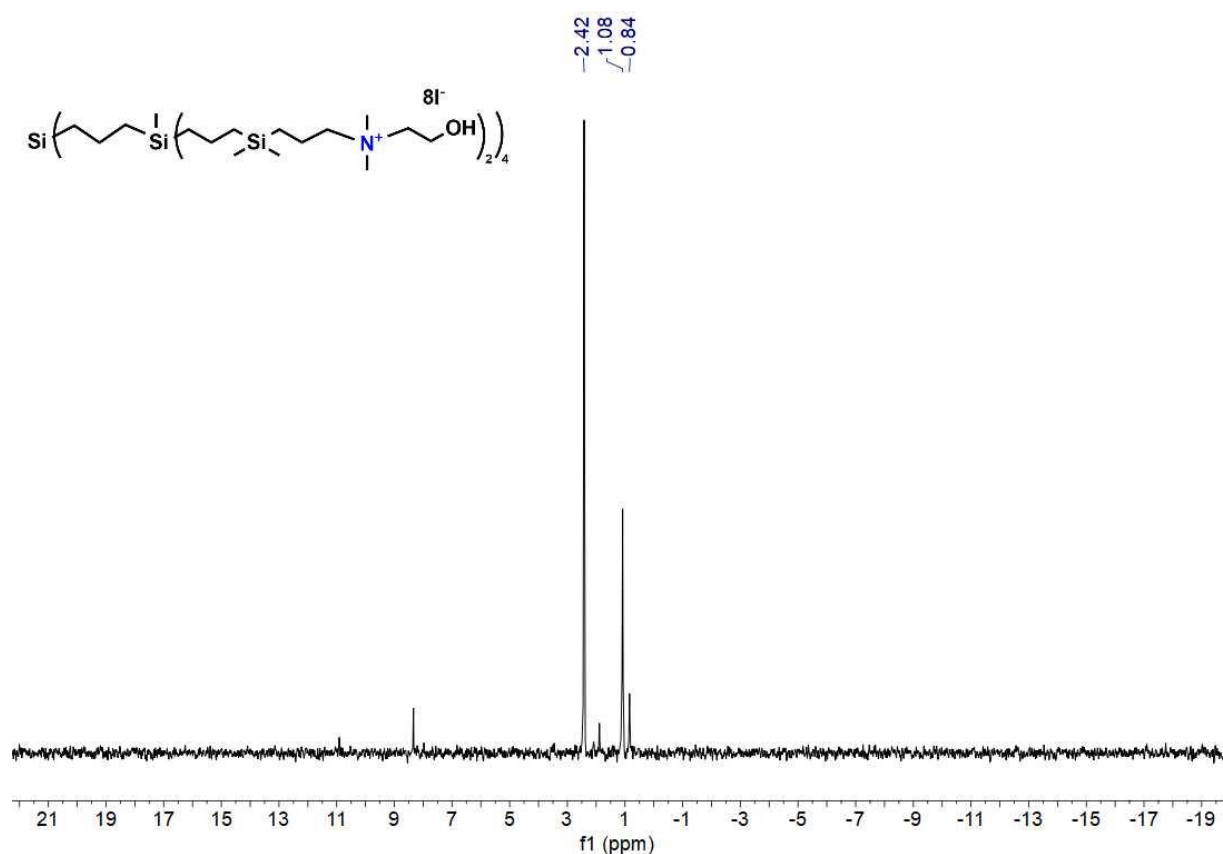


Figure S20. ^1H NMR spectrum of $\text{Dm}_3\text{AOH}_{16}$ in DMSO-d_6 .

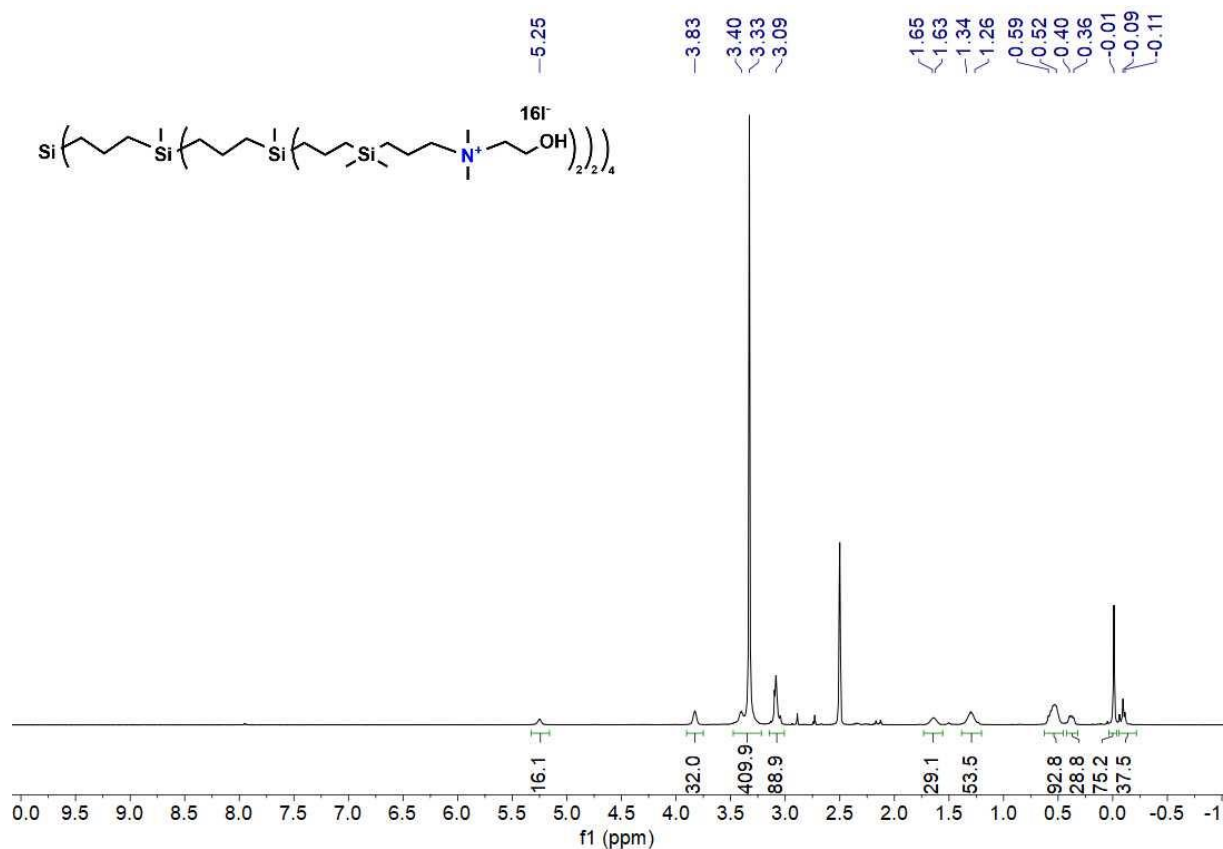


Figure S21. ^{13}C NMR spectrum of $\text{Dm}_3\text{AOH}_{16}$ in DMSO-d₆.

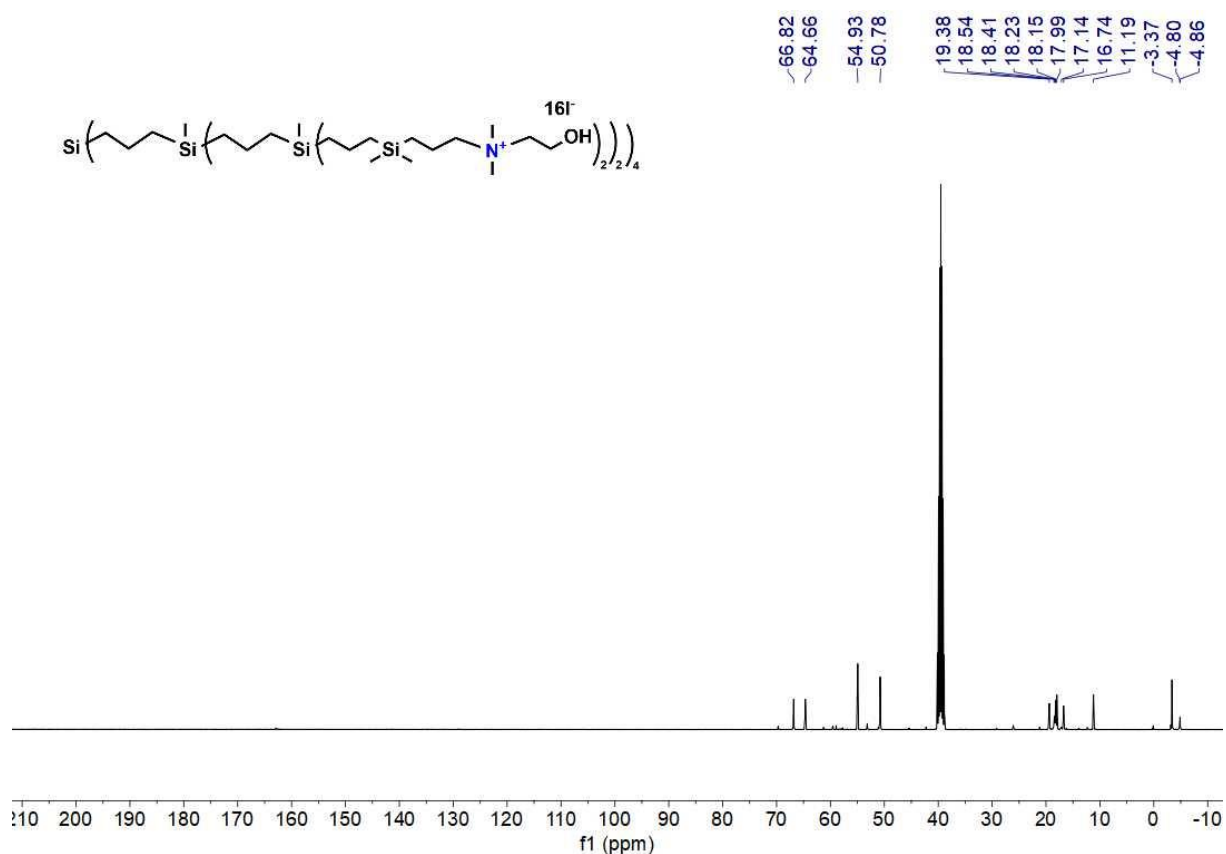


Figure S22. ^{29}Si NMR spectrum of $\text{Dm}_3\text{AOH}_{16}$ in DMSO-d₆.

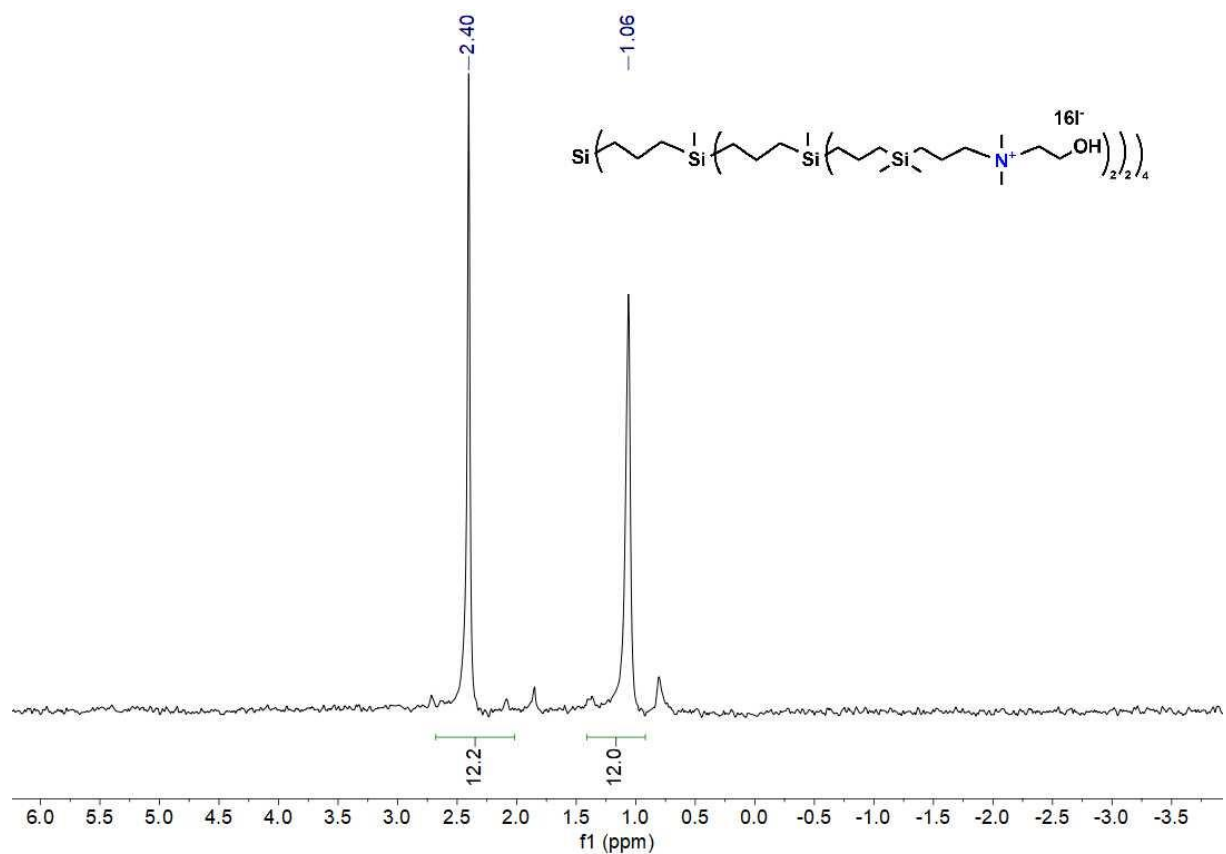


Figure S23. ^1H NMR spectrum of 4-(chloromethyl)-1,3-dioxolan-2-one in CDCl_3 .

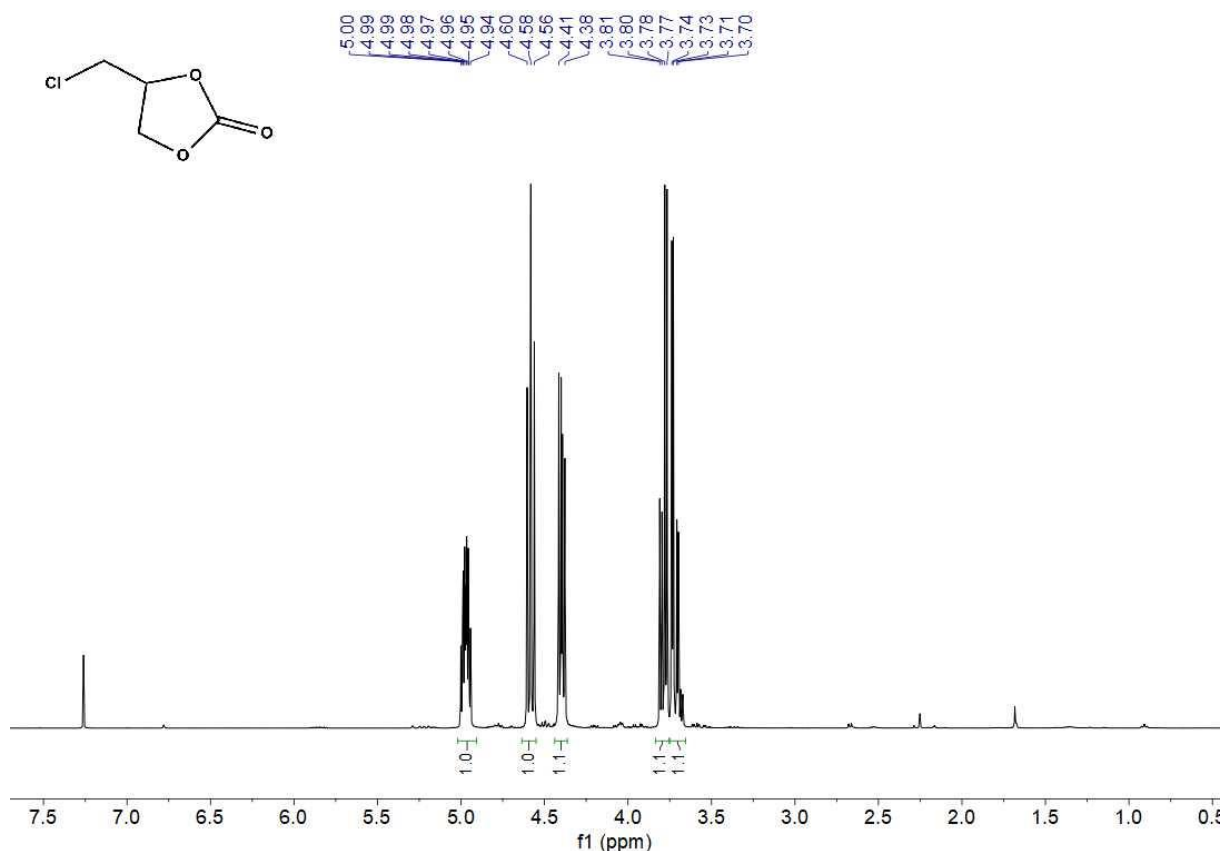


Figure S24. ^{13}C NMR spectrum of 4-(chloromethyl)-1,3-dioxolan-2-one in CDCl_3 .

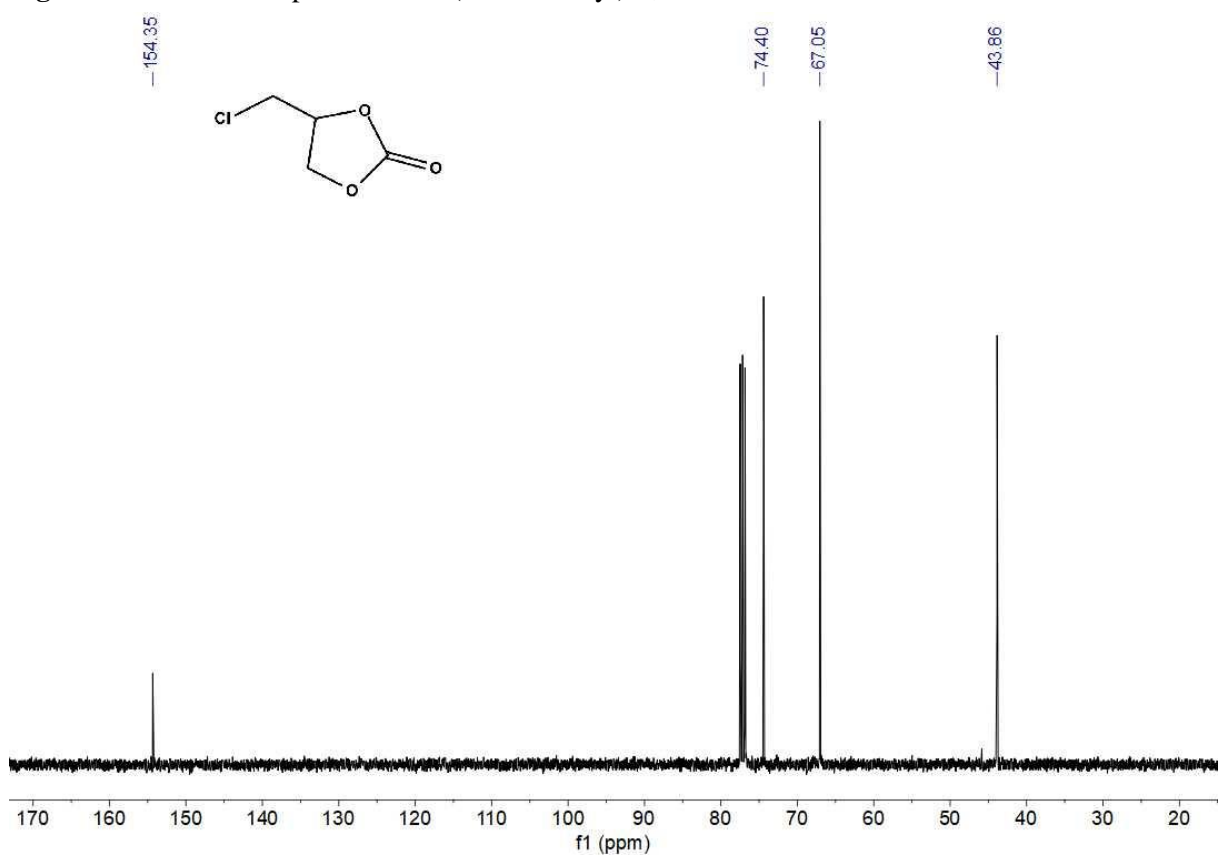


Figure S25. ^1H NMR spectrum of 4-butyl-1,3-dioxolan-2-one in CDCl_3 .

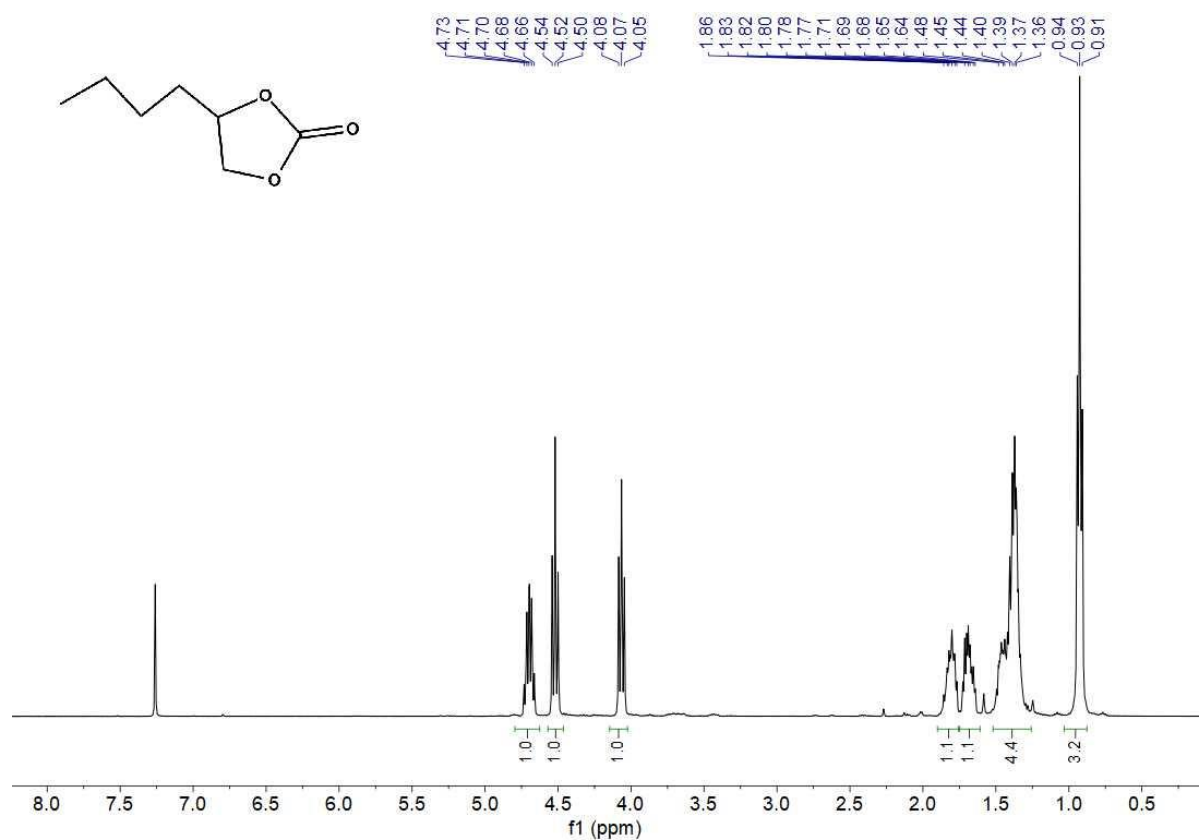


Figure S26. ^{13}C NMR spectrum of 4-butyl-1,3-dioxolan-2-one in CDCl_3 .

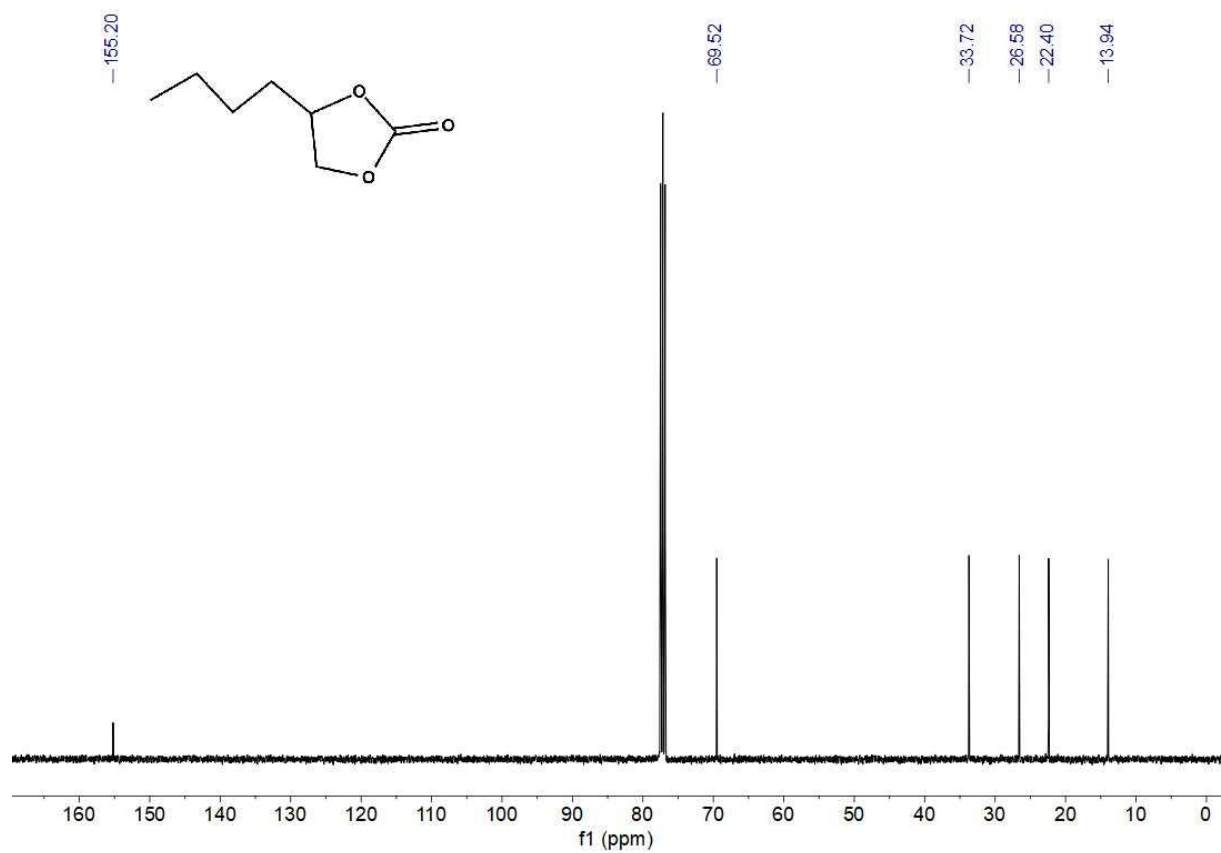


Figure S27. ^1H NMR spectrum of 4-(isopropoxymethyl)-1,3-dioxolan-2-one in CDCl_3 .

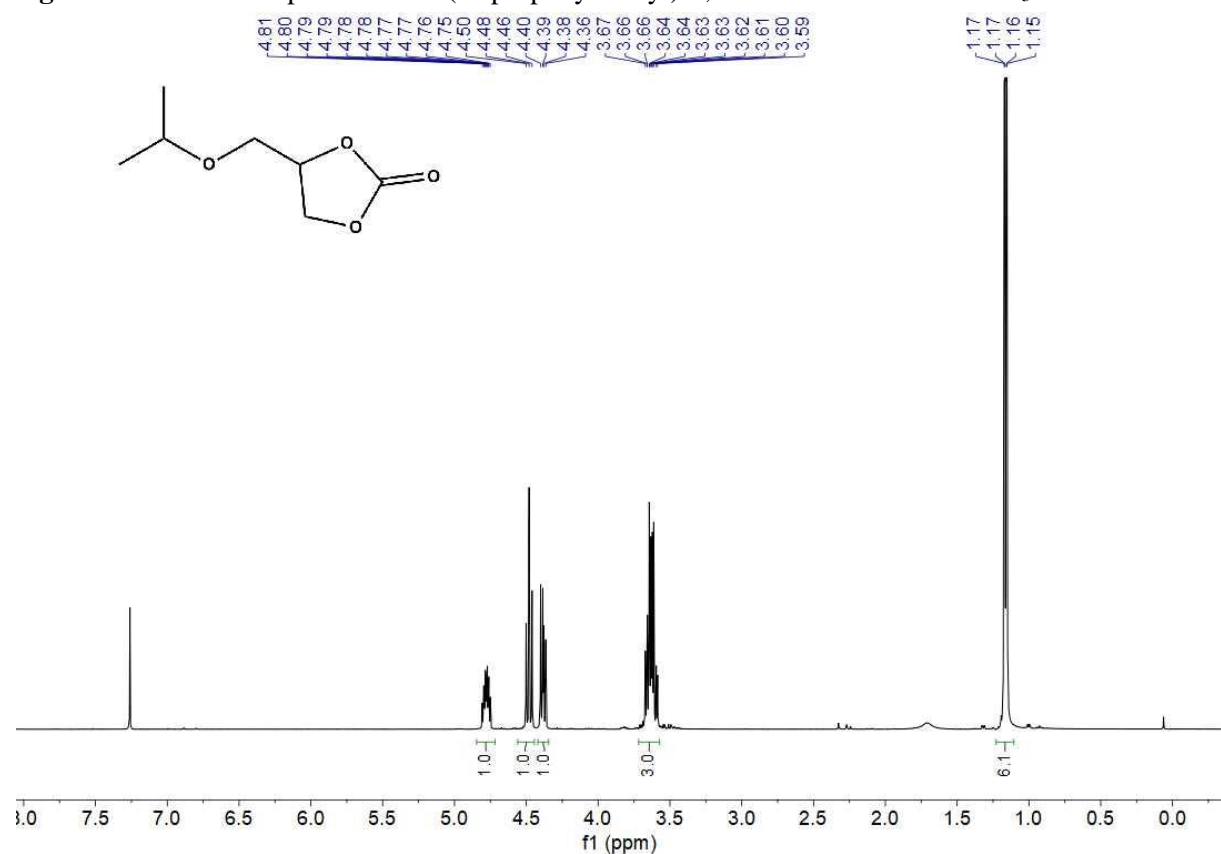


Figure S28. ^{13}C NMR spectrum of 4-(isopropoxymethyl)-1,3-dioxolan-2-one in CDCl_3 .

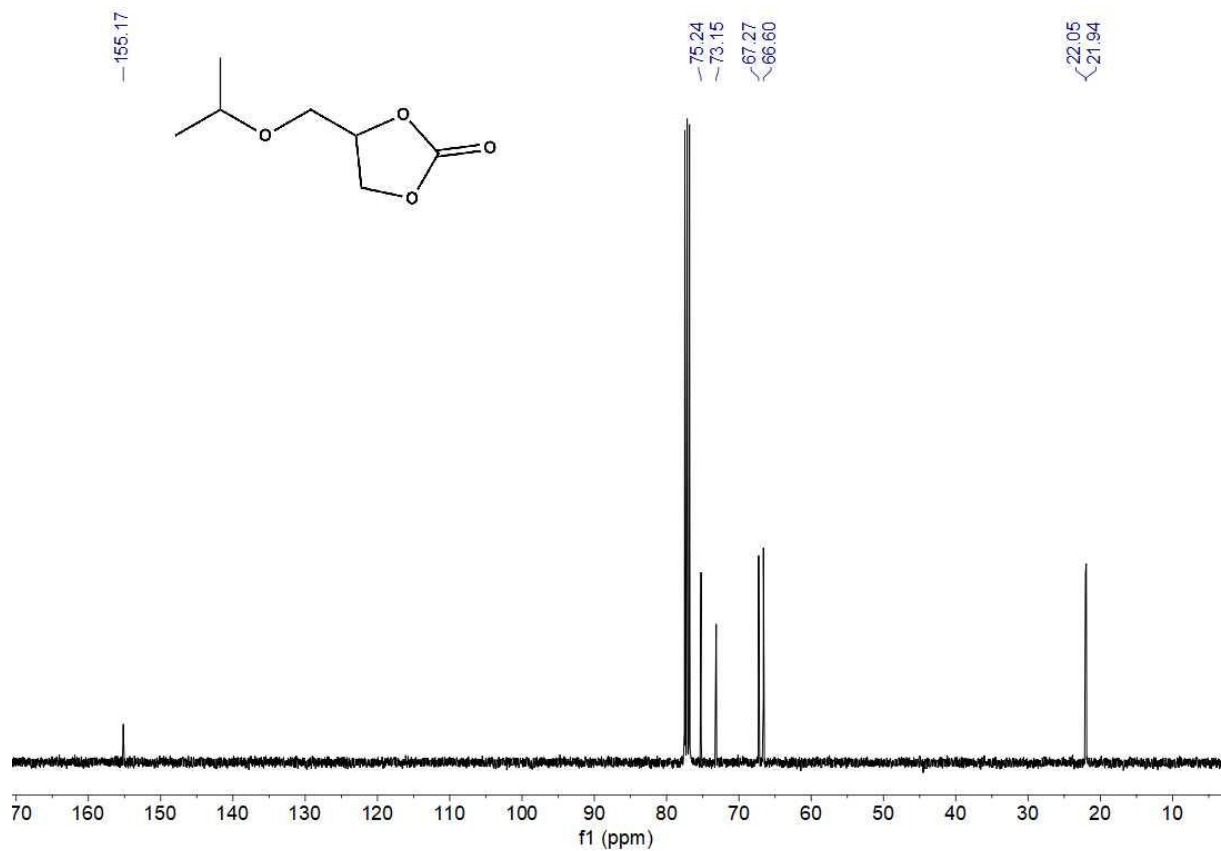


Figure S29. ^1H NMR spectrum of (2-oxo-1,3-dioxolan-4-yl)methyl methacrylate in CDCl_3 .

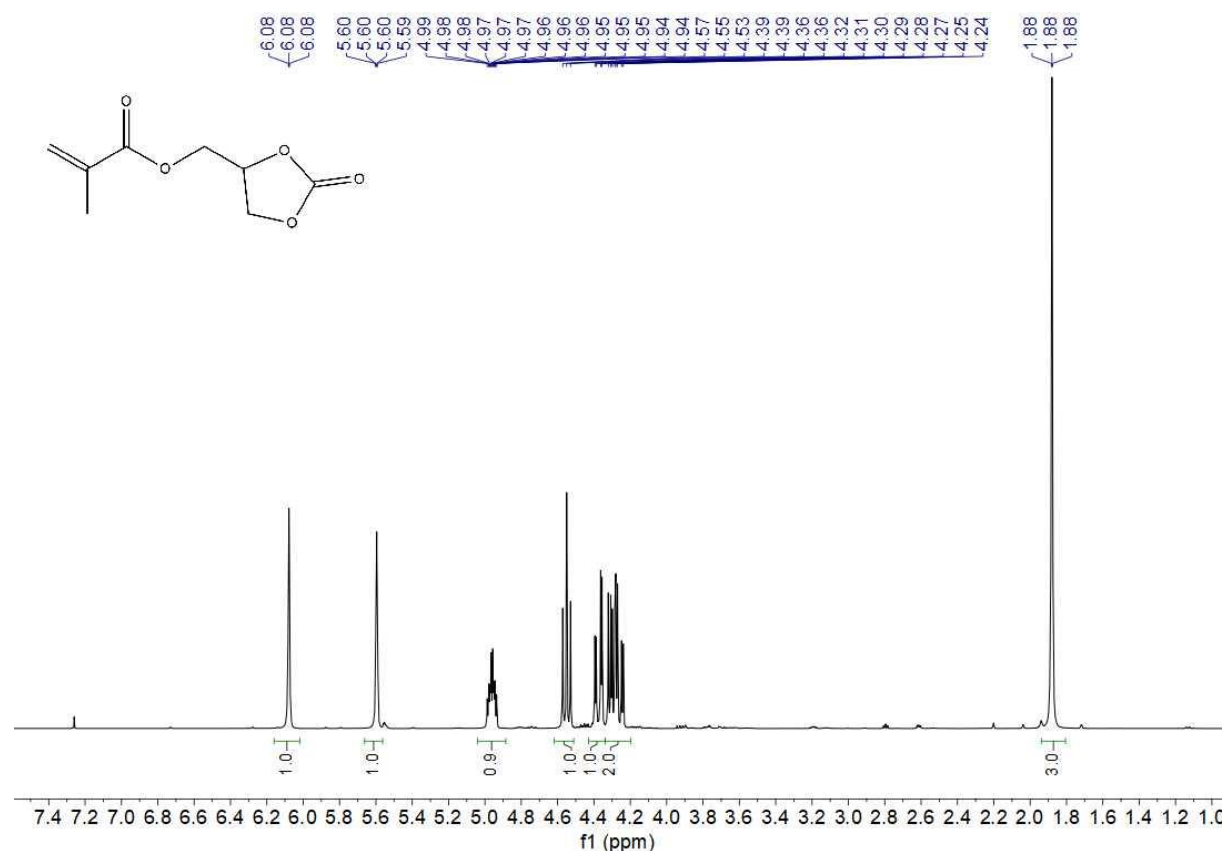
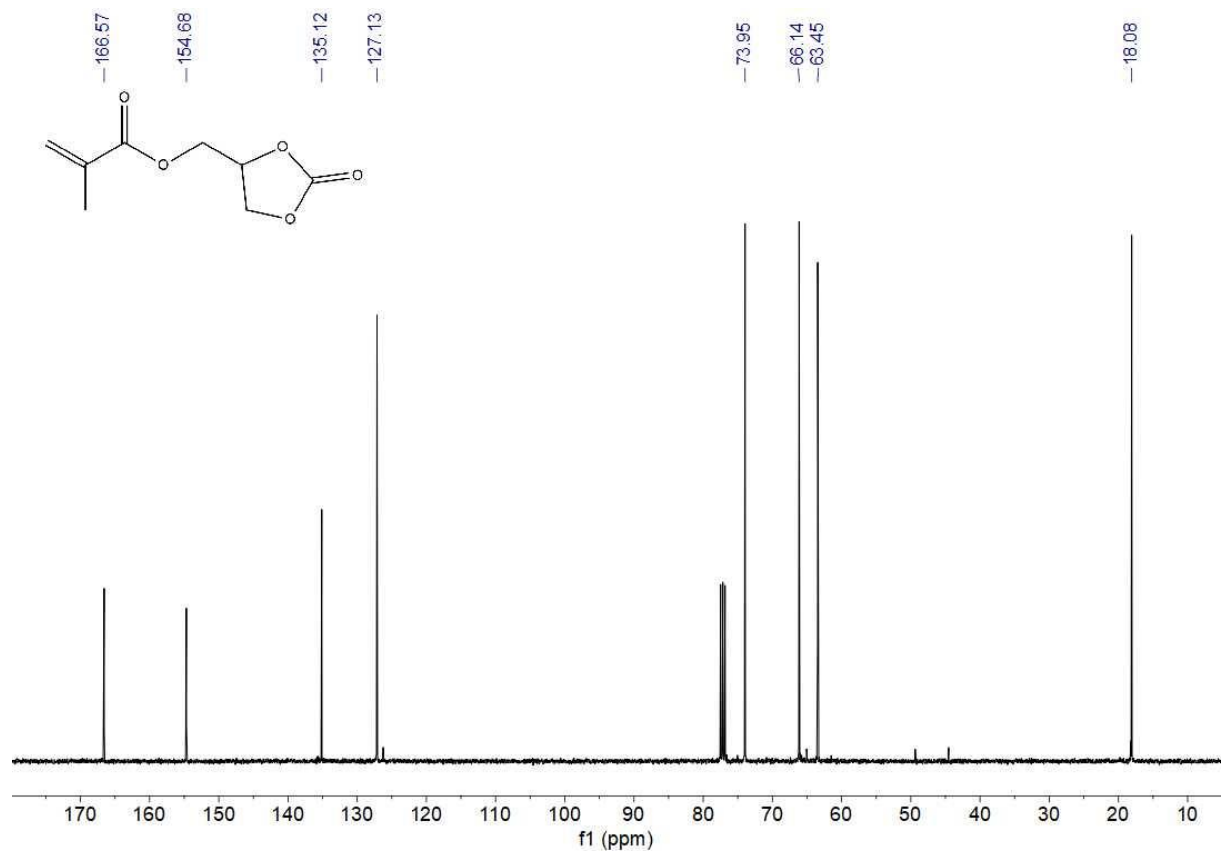


Figure S30. ^1H NMR spectrum of (2-oxo-1,3-dioxolan-4-yl)methyl methacrylate in CDCl_3 .



DFT Calculations

Geometry optimizations and frequency calculations have been performed with the Gaussian 09 program package³⁸. DFT calculations were carried out using the B3LYP^{39,40} gradient corrected hybrid density functional. As basis set we used LanL2DZ for iodine atom and 6-31+G(d,p) on all other atoms. No scaling factor has been used for the correction of the calculated wavenumbers.

The transition states (TS) were localized by the quadratic synchronous transit approach by Schlegel and co-workers⁴¹ (QST3) method as implemented in Gaussian09. Vibrational frequencies were calculated to confirm the saddle point order, evaluate free energies, and calculate the barriers to racemization.

Figure S31. Relative energy surface profiles obtained for the proposed step of cycloaddition catalyzed by Dm_0POH_1 and Dm_0NOH_1 .

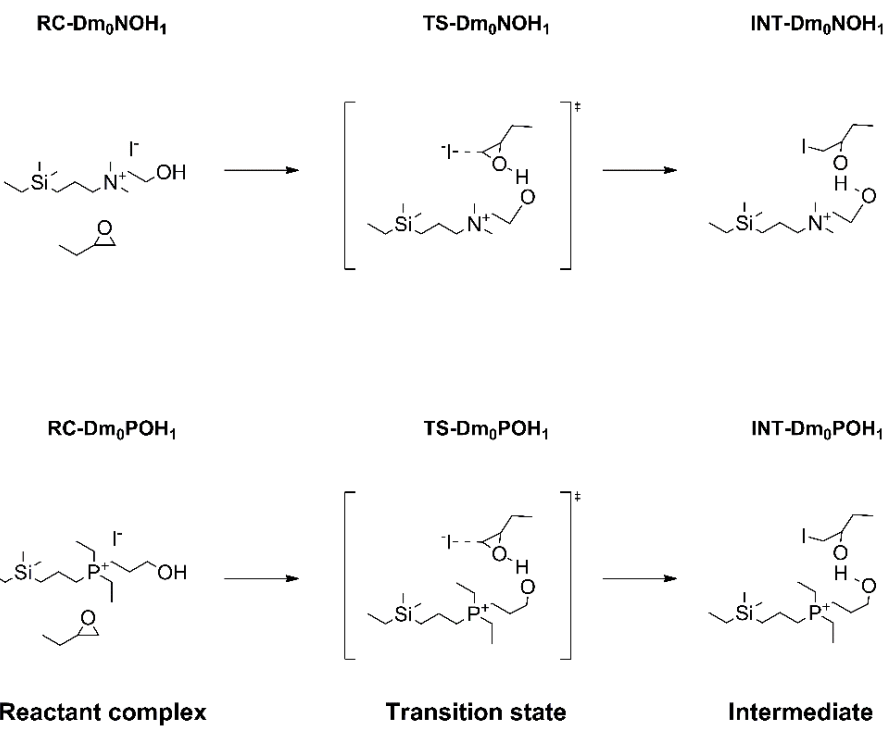
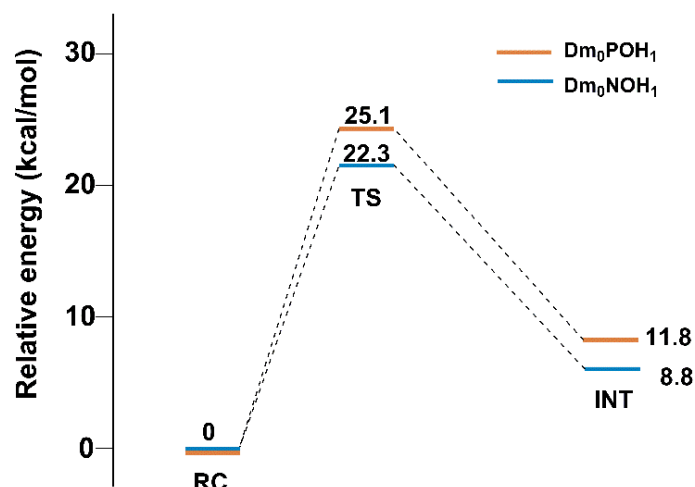


Table S3. Cartesian coordinates of reactant complex RC-Dm₀NOH₁.

HF = -1099.4104891

Symbol	X	Y	Z
C	1.4381790	3.4391000	-0.0695380
H	0.9157530	4.0661330	-0.7994680
H	1.2756540	3.8576720	0.9274160
C	-0.7757250	2.3735870	-0.1023060
H	-0.9445280	3.1318690	0.6695680
H	-0.9726350	2.8327460	-1.0762560
C	-1.6950100	1.1718310	0.1190230
H	-1.5680310	0.7892070	1.1360670
H	-1.4204190	0.3456300	-0.5431710
C	-3.1658020	1.5713060	-0.1078140
H	-3.2953300	1.9501110	-1.1328630
H	-3.4437460	2.4013290	0.5596990
C	-4.3445090	-0.4419080	1.9459420
H	-5.0981000	-1.2145250	2.1376680
H	-3.3673890	-0.8848460	2.1691640
H	-4.5206910	0.3754750	2.6559540
C	-4.0412150	-1.2701850	-1.0268630
H	-3.0487580	-1.6943330	-0.8320700
H	-4.7709290	-2.0807530	-0.9143880
H	-4.0687820	-0.9458990	-2.0744450
C	-6.1440900	0.8982140	-0.2182930
H	-6.2896710	1.7688800	0.4377530
H	-6.1258120	1.2991420	-1.2422560
Si	-4.4304470	0.1534390	0.1502040
C	-7.3368810	-0.0658950	-0.0658870
H	-7.4154150	-0.4515580	0.9570380
H	-8.2875060	0.4277000	-0.3006510
H	-7.2448090	-0.9291030	-0.7345790
C	2.9348940	3.4687730	-0.4047950
H	3.1911470	4.5372150	-0.4338850
H	3.1177830	3.0734620	-1.4102170
C	4.3050960	-1.0528810	-0.2851160
C	4.9888650	-0.5665310	-1.4909770
H	3.3224490	-1.5151690	-0.4093640
H	4.5341630	-0.7146310	-2.4690530
H	6.0724720	-0.4552150	-1.4855600
C	5.0603240	-1.4262050	0.9662560
H	5.2773760	-2.5011690	0.9008580
H	6.0255770	-0.9041040	0.9803870
C	4.2718440	-1.1404870	2.2519400
H	3.2988100	-1.6421120	2.2320640
H	4.8216190	-1.4938220	3.1303670
H	4.1024440	-0.0652760	2.3787840
O	4.2898190	0.3723580	-0.6411920
I	0.3966790	-2.2998930	-0.2680430
C	1.0887480	1.3012390	1.1609050
H	0.6176280	1.7883260	2.0170760
H	0.7374930	0.2722040	1.0402580
H	2.1686450	1.3234890	1.2759560
C	1.1121360	1.2974280	-1.3093570
H	0.8757420	1.8966850	-2.1917420

H	2.1755790	1.0658310	-1.2644860
H	0.5689470	0.3489640	-1.3044420
O	3.7551180	2.8406080	0.5574270
H	4.1281950	2.0183590	0.1854810
N	0.7309570	2.0886060	-0.0825480

Table S4. Cartesian coordinates of transition state TS-Dm₀NOH₁.

HF = -1099.37491465

Imaginary frequencies: -330.64

Symbol	X	Y	Z
C	0.5201350	3.2927220	-0.4849700
H	-0.0088360	3.8148120	-1.2885130
H	0.2947260	3.7832600	0.4657940
C	-1.6350380	2.1138480	-0.2549490
H	-1.7623410	2.7772970	0.6053560
H	-1.9502300	2.6582030	-1.1503790
C	-2.4792510	0.8492000	-0.0776030
H	-2.1529980	0.3026060	0.8125910
H	-2.3382410	0.1780400	-0.9308510
C	-3.9725790	1.2094980	0.0537410
H	-4.3029010	1.7632350	-0.8374050
H	-4.1181740	1.8911500	0.9045570
C	-4.6979050	-1.1966310	1.8810790
H	-5.3749250	-2.0403920	2.0569860
H	-3.6814580	-1.6047550	1.8398100
H	-4.7599060	-0.5373760	2.7551830
C	-4.9925920	-1.4458610	-1.1962650
H	-3.9846450	-1.8693380	-1.2744580
H	-5.6881290	-2.2885400	-1.1110120
H	-5.2149280	-0.9302620	-2.1382400
C	-6.9132320	0.4268600	0.3978900
H	-6.9371650	1.1554240	1.2210310
H	-7.1041880	1.0076800	-0.5160380
Si	-5.1538080	-0.2819900	0.2879410
C	-8.0378700	-0.6090910	0.5944610
H	-7.9058660	-1.1772890	1.5220850
H	-9.0211940	-0.1277970	0.6458450
H	-8.0720160	-1.3298310	-0.2301960
C	2.0358080	3.3688160	-0.7336450
H	2.2120350	4.4414760	-0.9355700
H	2.3108330	2.8436800	-1.6611090
C	4.3321290	0.2118200	0.5677080
C	3.6875010	-0.1896840	-0.6933560
H	3.6260830	0.4100380	1.3902770
H	2.8066330	0.3396370	-1.0010830
H	4.2970810	-0.6291660	-1.4720380
C	5.5024630	-0.6264640	1.0626480
H	5.1124120	-1.5905060	1.4127670
H	6.1642220	-0.8310360	0.2113690
C	6.2862190	0.0774130	2.1758540
H	5.6520280	0.2619410	3.0520080
H	7.1367280	-0.5298090	2.5043780
H	6.6688570	1.0423960	1.8280900

O	4.6869730	1.3658880	-0.1600030
I	1.9726380	-2.3332130	-0.4508790
C	0.4000580	1.1596410	0.8179390
H	-0.0485390	1.6087200	1.7058340
H	0.1502940	0.1029480	0.7343410
H	1.4771320	1.2970460	0.8559200
C	0.1492320	1.1201870	-1.6512710
H	-0.3224170	1.6337200	-2.4916120
H	1.2209020	1.0599380	-1.8107120
H	-0.2313070	0.1066920	-1.5438220
O	2.7665360	2.9277030	0.3663420
H	3.6064880	2.3702980	0.0986060
N	-0.1272980	1.9030960	-0.3958110

Table S5. Cartesian coordinates of intermediate INT-Dm₀NOH₁.

HF = -1099.39638879

Imaginary frequencies: -330.64

Symbol	X	Y	Z
C	-0.1402954	2.9084353	-1.2651933
H	-0.5797930	2.8570379	-2.2674825
H	-0.4836554	3.8193806	-0.7670683
C	-2.2367996	1.6733482	-0.8127628
H	-2.6281423	2.6895785	-0.7049599
H	-2.2735312	1.4141111	-1.8752217
C	-3.0923384	0.6942760	-0.0032616
H	-3.0775934	0.9705020	1.0561921
H	-2.6800056	-0.3178201	-0.0755870
C	-4.5467613	0.6943335	-0.5165357
H	-4.5605159	0.4552651	-1.5901426
H	-4.9699833	1.7057496	-0.4292705
C	-5.7956461	-0.1186154	2.2130577
H	-6.4979461	-0.7774310	2.7364278
H	-4.8167223	-0.2486534	2.6891038
H	-6.1188725	0.9142276	2.3895944
C	-5.1153695	-2.2945008	0.1158755
H	-4.1322451	-2.4503321	0.5751533
H	-5.8013172	-3.0173831	0.5722354
H	-5.0311514	-2.5472387	-0.9478258
C	-7.4460544	-0.2945177	-0.4301220
H	-7.7346340	0.7608398	-0.3209865
H	-7.3435772	-0.4610586	-1.5121056
Si	-5.7346654	-0.5208943	0.3623514
C	-8.5666826	-1.1953432	0.1254784
H	-8.7285174	-1.0262366	1.1960647
H	-9.5202402	-1.0055883	-0.3803868
H	-8.3351187	-2.2580489	-0.0080200
C	1.4091816	2.8640989	-1.3319119
H	1.6672941	3.8360291	-1.8152696
H	1.6742323	2.0977390	-2.1022749
C	4.3650179	0.6576164	0.5358520
C	4.1283174	-0.1527943	-0.7471604
H	3.5013110	0.5205710	1.2069948
H	3.3467821	0.2990752	-1.3533185

H	5.0365825	-0.2791831	-1.3372406
C	5.6437168	0.2474676	1.2708131
H	5.6153950	-0.8311308	1.4692702
H	6.4910640	0.4312577	0.5962112
C	5.8489169	1.0174008	2.5794357
H	5.0346387	0.8166756	3.2870863
H	6.7888408	0.7290385	3.0636410
H	5.8722651	2.0943340	2.3902854
O	4.4662501	2.0020036	0.1285334
I	3.3786067	-2.2279575	-0.3968187
C	-0.5729453	2.0637315	1.0173927
H	-1.2178592	2.9064015	1.2754590
H	-0.8478816	1.1851020	1.6017207
H	0.4873749	2.3250015	1.1256067
C	-0.0588253	0.4637598	-0.7724830
H	-0.1306931	0.2774753	-1.8449807
H	0.9802470	0.5797682	-0.4652216
H	-0.5297516	-0.3465864	-0.2183063
O	1.9886673	2.6527608	-0.1218826
H	3.5177635	2.3507053	-0.0121587
N	-0.7621173	1.7563994	-0.4526856

Table S6. Cartesian coordinates of reactant complex RC-Dm₀POH₁.

HF = -1504.00027414

Symbol	X	Y	Z
C	-0.4608723	1.3624559	1.5156730
H	-1.5068417	1.6666079	1.6350964
H	-0.4788636	0.2792583	1.3331488
C	0.5422544	3.8448551	0.2256458
H	1.3995793	3.8214958	0.9073523
H	-0.2814965	4.3097603	0.7799036
C	-1.2828668	2.0445454	-1.3278387
H	-0.7756823	2.2915832	-2.2681453
H	-1.5467359	0.9782575	-1.3941914
C	1.4446964	1.1875653	-0.8559193
H	0.9687727	0.2851608	-1.2675252
H	1.7937924	1.7999625	-1.6972730
C	2.6211050	0.7674257	0.0442526
H	2.2353030	0.1195099	0.8381732
H	3.0727468	1.6433139	0.5295101
C	3.6880733	0.0035473	-0.7633036
H	4.1038635	0.6602411	-1.5421397
H	3.1992054	-0.8256010	-1.2937605
C	4.4558759	-1.9142511	1.5567032
H	5.2671296	-2.4219475	2.0909553
H	3.8563663	-1.3827063	2.3049511
H	3.8149366	-2.6822383	1.1086739
C	6.1133847	0.6581936	1.0776308
H	5.4875246	1.2255056	1.7770715
H	6.9589304	0.2597168	1.6501848
H	6.5162075	1.3644040	0.3413697
C	6.2454241	-1.6661177	-0.9914313
H	5.6257154	-2.4167174	-1.5020544

H	6.5513816	-0.9558567	-1.7733410
Si	5.1330936	-0.7351624	0.2390460
P	0.0557733	2.0949493	-0.0770770
C	7.4930142	-2.3454961	-0.3944623
H	7.2224773	-3.0974120	0.3554878
H	8.0808887	-2.8556480	-1.1666202
H	8.1561536	-1.6204792	0.0918058
C	-2.5337237	2.9364918	-1.1376944
H	-2.8271234	3.3156721	-2.1243511
H	-2.3218262	3.8227829	-0.5257796
C	0.3815421	1.7360864	2.7450434
H	-0.0182923	1.2048740	3.6142290
H	1.4322800	1.4504960	2.6444172
H	0.3358715	2.8062360	2.9716988
C	0.8772556	4.6611798	-1.0323093
H	0.0198989	4.7401251	-1.7071120
H	1.1670045	5.6770081	-0.7466797
H	1.7115690	4.2266198	-1.5910993
I	-0.9319832	-1.8634629	-0.6997365
C	-4.8063664	-1.7607383	0.5428282
C	-4.1923198	-1.7138770	1.8729537
H	-4.1122442	-1.7275100	-0.2984904
H	-3.1069023	-1.6764397	1.9396041
H	-4.7244287	-2.1285030	2.7280834
C	-6.1569017	-2.3816047	0.2850782
H	-5.9935267	-3.4319100	0.0073278
H	-6.7363281	-2.3812791	1.2165355
C	-6.9386407	-1.6643294	-0.8242027
H	-6.3820143	-1.6729815	-1.7684254
H	-7.9043375	-2.1494794	-1.0013887
H	-7.1305189	-0.6206230	-0.5531672
O	-4.8136132	-0.5244270	1.3200451
C	-3.7416044	2.2111299	-0.5441167
H	-4.6171484	2.8759888	-0.6091358
H	-3.9572018	1.3145641	-1.1412701
O	-3.4875509	1.8639022	0.8074523
H	-3.9475513	1.0215855	1.0147487

Table S7. Cartesian coordinates of transition state TS-Dm₀POH₁.

HF = - 1503.96030474

Imaginary frequencies: -394.38

Symbol	X	Y	Z
C	2.3539532	-0.9928092	1.7019148
H	3.3199020	-0.5352616	1.9384602
H	1.6669389	-0.1499622	1.5849289
C	3.0317340	-3.4713165	0.2011262
H	2.2598142	-3.9648027	0.8015690
H	3.9445462	-3.4721268	0.8088420
C	3.7602290	-0.8239314	-0.9936798
H	3.8797134	-1.4308488	-1.8982279
H	3.2479485	0.1022559	-1.2819243
C	0.9417801	-1.6007628	-0.9054513
H	0.8625329	-0.5342185	-1.1442634

H	1.0819176	-2.1322549	-1.8548202
C	-0.3378981	-2.0830723	-0.1899564
H	-0.4109055	-1.5935409	0.7876837
H	-0.2758575	-3.1626827	0.0019374
C	-1.5987181	-1.7576267	-1.0110778
H	-1.5360475	-2.2425825	-1.9965747
H	-1.6358825	-0.6757981	-1.2012618
C	-3.3498873	-1.5539016	1.5537652
H	-4.3317537	-1.7454629	2.0023370
H	-2.6017496	-2.0214488	2.2060799
H	-3.1851079	-0.4696159	1.5606513
C	-3.4285360	-4.1220806	-0.1839950
H	-2.6317936	-4.5857919	0.4109565
H	-4.3826535	-4.4349983	0.2559984
H	-3.3785746	-4.5429506	-1.1957711
C	-4.6312703	-1.4621418	-1.2925794
H	-4.4588475	-0.3773733	-1.3111335
H	-4.4855060	-1.8095241	-2.3260208
Si	-3.2744780	-2.2267816	-0.2104445
P	2.5188324	-1.7123792	0.0217179
C	-6.0790018	-1.7493583	-0.8493283
H	-6.2736832	-1.3631105	0.1573539
H	-6.8034592	-1.2751714	-1.5216580
H	-6.2976605	-2.8239403	-0.8400047
C	5.1293470	-0.5047491	-0.3406618
H	5.9246960	-0.7431876	-1.0578341
H	5.3190276	-1.1307823	0.5409601
C	1.8959542	-1.9528643	2.8110096
H	1.7802370	-1.3831594	3.7376680
H	0.9322749	-2.4228634	2.5953847
H	2.6288604	-2.7421024	3.0035597
C	3.2574581	-4.2344175	-1.1129544
H	4.0602371	-3.7945527	-1.7116349
H	3.5432550	-5.2667777	-0.8905308
H	2.3525653	-4.2708367	-1.7268973
I	-2.4581500	2.7059575	0.4516848
C	0.9922971	2.5152104	-0.7774601
C	0.3221252	1.9224143	0.3736083
H	0.5863978	2.2166861	-1.7533175
H	-0.1780916	0.9746678	0.2833245
H	0.4673693	2.3488140	1.3559589
C	1.3675782	3.9852111	-0.7497585
H	0.4480704	4.5647396	-0.8953581
H	1.7477852	4.2306202	0.2500693
C	2.4081795	4.3488543	-1.8150024
H	2.0330932	4.1384040	-2.8241637
H	2.6605547	5.4134842	-1.7714312
H	3.3345748	3.7802506	-1.6741849
O	1.9642974	1.5968455	-0.2766809
C	5.2672012	0.9758075	0.0619100
H	6.2689938	1.1333085	0.4788907
H	5.1838431	1.6024934	-0.8390267
O	4.3324324	1.3737270	1.0438538
H	3.4855912	1.6415163	0.6086276

Table S8. Cartesian coordinates of intermediate INT-Dm₀POH₁.

HF = -1503.98139432

Symbol	X	Y	Z
C	0.3004670	-2.2755790	1.7814180
H	1.2205480	-2.8270060	1.9995270
H	0.6436950	-1.2615630	1.5488130
C	-1.4650920	-4.2982610	0.5157460
H	-2.2399620	-3.9199690	1.1910230
H	-0.8919470	-5.0387060	1.0871330
C	1.0125480	-3.5046700	-0.9393950
H	0.4886060	-4.0364330	-1.7417610
H	1.4333800	-2.5783020	-1.3545020
C	-1.1771220	-1.5796630	-0.7570670
H	-0.3501600	-0.8942860	-0.9922090
H	-1.5326630	-2.0208930	-1.6968750
C	-2.3182110	-0.8440200	-0.0307840
H	-1.9185580	-0.3800960	0.8785170
H	-3.0897920	-1.5557530	0.2920190
C	-2.9551060	0.2402380	-0.9220680
H	-3.3832980	-0.2287810	-1.8204470
H	-2.1667380	0.9149780	-1.2848190
C	-3.5661220	2.2724780	1.3509390
H	-4.3129070	2.9266410	1.8157190
H	-3.1940550	1.6003430	2.1332090
H	-2.7279310	2.9015200	1.0293620
C	-5.7067020	0.1953790	0.5263950
H	-5.3457400	-0.5114120	1.2831910
H	-6.5068950	0.7840090	0.9896960
H	-6.1539240	-0.3868840	-0.2883940
C	-4.9607820	2.5053440	-1.4306090
H	-4.1069120	3.0780290	-1.8197060
H	-5.3219640	1.9040620	-2.2774910
Si	-4.3071640	1.3122560	-0.1040200
P	-0.3123170	-2.8999690	0.1704980
C	-6.0685950	3.4753780	-0.9759240
H	-5.7263580	4.1274280	-0.1642720
H	-6.3950590	4.1245430	-1.7966810
H	-6.9536090	2.9387490	-0.6149310
C	2.1335050	-4.3724350	-0.3153290
H	2.3635680	-5.1957200	-1.0042270
H	1.8127590	-4.8412410	0.6249640
C	-0.6859960	-2.3274680	2.9571760
H	-0.2159740	-1.8567110	3.8262010
H	-1.6169050	-1.7879070	2.7582970
H	-0.9410840	-3.3526570	3.2437490
C	-2.1084550	-4.9522350	-0.7167140
H	-1.3617300	-5.3801630	-1.3918760
H	-2.7684910	-5.7656590	-0.3999510
H	-2.7145080	-4.2409260	-1.2861200
I	2.6388510	3.5415610	0.4699260
C	2.2195250	0.5800510	-0.7377820
C	2.3877580	1.3123490	0.6031690
H	1.4246130	1.1070200	-1.3096800
H	1.4919900	1.2090620	1.2125610

H	3.2653790	0.9712830	1.1539850
C	3.5014590	0.6223650	-1.5932140
H	3.8109170	1.6641150	-1.7439210
H	4.3029260	0.1254230	-1.0281760
C	3.3269200	-0.0591790	-2.9538150
H	2.5457080	0.4369640	-3.5445370
H	4.2536450	-0.0296420	-3.5386160
H	3.0368310	-1.1081230	-2.8304420
O	1.8266080	-0.7092450	-0.4070380
C	3.4209850	-3.5604950	-0.0613660
H	4.1793860	-4.2318750	0.3631410
H	3.8057930	-3.2074450	-1.0332140
O	3.2304780	-2.4926390	0.8295420
H	2.7807930	-1.7132130	0.3397820

References

- Steinbauer, J.; Kubis, C.; Ludwig, R.; Werner, T. Mechanistic Study on the Addition of CO₂ to Epoxides Catalyzed by Ammonium and Phosphonium Salts: A Combined Spectroscopic and Kinetic Approach. *ACS Sustainable Chem. Eng.* **2018**, 6 (8), 10778–10788.
- Kohrt, C.; Werner, T. Recyclable Bifunctional Polystyrene and Silica Gel-Supported Organocatalyst for the Coupling of CO₂ with Epoxides. *ChemSusChem* **2015**, 8 (12), 2031–2034.
- Büttner, H.; Steinbauer, J.; Werner, T. Synthesis of Cyclic Carbonates from Epoxides and Carbon Dioxide by Using Bifunctional One-Component Phosphorus-Based Organocatalysts. *ChemSusChem* **2015**, 8 (16), 2655–2669.
- Peng, J. J.; Deng, Y. Q. Cycloaddition of carbon dioxide to propylene oxide catalyzed by ionic liquids. *New J. Chem.* **2001**, 25 (4), 639–641.
- Zhang, Y.; Yin, S.; Luo, S.; Au, C. T. Cycloaddition of CO₂ to Epoxides Catalyzed by Carboxyl-Functionalized Imidazolium-Based Ionic Liquid Grafted onto Cross-Linked Polymer. *Ind. Eng. Chem. Res.* **2012**, 51 (10), 3951–3957.
- Dai, W. L.; Chen, L.; Yin, S. F.; Li, W. H.; Zhang, Y. Y.; Luo, S. L.; Au, C. T. High-Efficiency Synthesis of Cyclic Carbonates from Epoxides and CO₂ over Hydroxyl Ionic Liquid Catalyst Grafted onto Cross-Linked Polymer. *Catal. Lett.* **2010**, 137, 74–80.
- Anthofer, M. H.; Wilhelm, M. E.; Cokoja, M.; Drees, M.; Herrmann, W. A.; Kühn, F. E. Hydroxy-Functionalized Imidazolium Bromides as Catalysts for the Cycloaddition of CO₂ and Epoxides to Cyclic Carbonates. *ChemCatChem* **2015**, 7 (1), 94–98.
- Wang, T.; Zheng, D.; Zhang, J.; Fan, B.; Ma, Y.; Ren, T.; Wang, L.; Zhang, J. Protic Pyrazolium Ionic Liquids: An Efficient Catalyst for Conversion of CO₂ in the Absence of Metal and Solvent. *ACS Sustainable Chem. Eng.* **2018**, 6 (2), 2574–2582.
- Zhou, Y.; Hu, S.; Ma, X.; Liang, S.; Jiang, T.; Han, B. Synthesis of cyclic carbonates from carbon dioxide and epoxides over betaine-based catalysts. *J. Mol. Catal. A: Chem.* **2008**, 284, 52–57.
- Watle, R. A.; Deshmukh, K. M.; Dhake, K. P.; Bhanage, B. M. Efficient synthesis of cyclic carbonate from carbon dioxide using polymer anchored diol functionalized ionic liquids as a highly active heterogeneous catalyst *Catal. Sci. Technol.* **2012**, 2 (5), 1051–1055.
- Dai, W. L.; Jin, B.; Luo, S. L.; Luo, X. B.; Tu, X. M.; Au, C. T. Novel functionalized guanidinium ionic liquids: Efficient acid-base bifunctional catalysts for CO₂ fixation with epoxides. *J. Mol. Catal. A: Chem.* **2013**, 378, 326–332.

12. Liu, Y.; Cheng, W.; Zhang, Y.; Sun, J.; Zhang, S. Controllable Preparation of Phosphonium-Based Polymeric Ionic Liquids as Highly Selective Nanocatalysts for the Chemical Conversion of CO₂ with Epoxides. *Green Chem.* **2017**, *19* (9), 2184–2193.
13. Liu, M.; Liang, L.; Li, X.; Gao, X.; Sun, J. Novel urea derivative-based ionic liquids with dual-functions: CO₂ capture and conversion under metal- and solvent-free conditions. *Green Chem.* **2016**, *18* (9), 2851–2863.
14. Sun, J.; Zhang, S.; Cheng, W.; Ren, J. Hydroxyl-functionalized ionic liquid: a novel efficient catalyst for chemical fixation of CO₂ to cyclic carbonate. *Tetrahedron Lett.* **2008**, *49* (22), 3588–3591.
15. Kim, H. S.; Kim, J. J.; Kim, H.; Jang, H. G. Imidazolium zinc tetrahalide-catalyzed coupling reaction of CO₂ and ethylene oxide or propylene oxide. *J. Catal.* **2003**, *220*, 44–46.
16. Wu, S.; Wang, B.; Zhang, Y.; Elageed, E. H. M.; Wu, H.; Gao, G. Phenolic Hydroxyl-Functionalized Imidazolium Ionic Liquids: Highly Efficient Catalysts for the Fixation of CO₂ to Cyclic Carbonates. *J. Mol. Catal. A: Chem.* **2016**, *418–419*, 1–8.
17. Wang, J. Q.; Cheng, W. G.; Sun, J.; Shi, T. Y.; Zhang, X. P.; Zhang, S. J. Efficient fixation of CO₂ into organic carbonates catalyzed by 2-hydroxymethyl-functionalized ionic liquids *RSC Adv.* **2014**, *4* (5), 2360–2367.
18. Roshan, K. R.; Jose, T.; Kathalikkattil, A. C.; Kim, D. W.; Kim, B.; Park, D. W. Microwave synthesized quaternized celluloses for cyclic carbonate synthesis from carbon dioxide and epoxides. *Appl. Catal. A – Gen.* **2013**, *467*, 17–25.
19. Lee, S. D.; Kim, B. M.; Kim, D. W.; Kim, M. I.; Roshan, K. R.; Kim, M. K.; Won, Y. S.; Park, D. W. Synthesis of Cyclic Carbonate from Carbon Dioxide and Epoxides with Polystyrene-Supported Quaternized Ammonium Salt Catalysts. *Appl. Catal. A – Gen.* **2014**, *486*, 69–76.
20. Tharun, J.; Mathai, G.; Roshan, R.; Kathalikkattil, A. C.; Bomu, K.; Park, D. W. Simple and efficient synthesis of cyclic carbonates using quaternized glycine as a green catalyst. *Phys. Chem. Chem. Phys.* **2013**, *15* (23), 9029–9033.
21. Xiao, L. F.; Li, F. W.; Xia, C. G. An easily recoverable and efficient natural biopolymer-supported zinc chloride catalyst system for the chemical fixation of carbon dioxide to cyclic carbonate. *Appl. Catal. A – Gen.* **2005**, *279*, 125–129.
22. Han, L.; Choi, H. J.; Choi, S. J.; Liu, B.; Park, D. W. Ionic liquids containing carboxyl acid moieties grafted onto silica: Synthesis and application as heterogeneous catalysts for cycloaddition reactions of epoxide and carbon dioxide. *Green Chem.* **2011**, *13* (4), 1023–1028.
23. Roshan, K. R.; Mathai, G.; Kim, J.; Tharun, J.; Park, G. A.; Park, D. W. A biopolymer mediated efficient synthesis of cyclic carbonates from epoxides and carbon dioxide. *Green Chem.* **2012**, *14* (10), 2933–2940.
24. Zhu, A.; Jiang, T.; Han, B.; Zhang, J.; Xie, Y.; Ma, X. Supported Choline Chloride/Urea as a Heterogeneous Catalyst for Chemical Fixation of Carbon Dioxide to Cyclic Carbonates. *Green Chem.* **2007**, *9* (2), 169–172.
25. Dou, X. Y.; Wang, J. Q.; Du, Y.; Wang, E.; He, N. L. Guanidinium salt functionalized PEG: An effective and recyclable homogeneous catalyst for the synthesis of cyclic carbonates from CO₂ and epoxides under solvent-free conditions. *Synlett* **2007**, 3058–3062.
26. Li, F.; Xiao, L.; Xia, C.; Hu, B. Chemical fixation of CO₂ with highly efficient ZnCl₂/[BmIm]Br catalyst system. *Tetrahedron Lett.* **2004**, *45* (45), 8307–8310.
27. Ono, F.; Qiao, K.; Tomida, D.; Yokoyama, C. Rapid synthesis of cyclic carbonates from CO₂ and epoxides under microwave irradiation with controlled temperature and pressure. *J. Mol. Catal. A: Chem.* **2007**, *263*, 223–226.
28. Sun, J.; Han, L.; Cheng, W.; Wang, J.; Zhang, X.; Zhang, S. Efficient Acid-Base Bifunctional

- Catalysts for the Fixation of CO₂ with Epoxides under Metal- and Solvent-Free Conditions. *ChemSusChem* **2011**, *4* (4), 502–507.
- 29. Wang, J. Q.; Dong, K.; Cheng, W. G.; Sun, J.; Zhang, S. J. Insights into quaternary ammonium salts-catalyzed fixation carbon dioxide with epoxides. *Catal. Sci. Technol.* **2012**, *2* (7), 1480–1484.
 - 30. Sopeña, S.; Martin, E.; Escudero-Adán, E. C.; Kleij, A. W. Pushing the Limits with Squaramide-Based Organocatalysts in Cyclic Carbonate Synthesis. *ACS Catal.* **2017**, *7* (5), 3532–3539.
 - 31. Foltran, S.; Alsarraf, J.; Robert, F.; Landais, Y.; Cloutet, E.; Cramail, H.; Tassaing, T. On the chemical fixation of supercritical carbon dioxide with epoxides catalyzed by ionic salts: an in situ FTIR and Raman study. *Catal. Sci. Technol.* **2013**, *3* (4), 1046–1055.
 - 32. Chen, Y.; Luo, R.; Bao, J.; Xu, Q.; Jiang, J.; Zhou, X.; Ji, H. Function-oriented ionic polymers featuring high-density active sites for sustainable carbon dioxide conversion. *J. Mater. Chem. A* **2018**, *6* (19), 9172–9182.
 - 33. Liu, X.; Zhi, Y.; Shao, P.; Feng, X.; Xia, H.; Zhang, Y.; Shi, Z.; Mu, Y. Covalent organic frameworks: efficient, metal-free, heterogeneous organocatalysts for chemical fixation of CO₂ under mild conditions. *J. Mater. Chem. A* **2018**, *6* (2), 374–382.
 - 34. Subramanian, S.; Park, J.; Byun, J.; Jung, Y.; Yavuz, C. T. Highly Efficient Catalytic Cyclic Carbonate Formation by Pyridyl Salicylimines. *ACS Appl. Mater. Interfaces* **2018**, *10* (11), 9478–9484.
 - 35. Jose, T.; Cañellas, S.; Pericàs, M. A.; Kleij, A. W. Polystyrene-supported bifunctional resorcinarenes as cheap, metal-free and recyclable catalysts for epoxide/CO₂ coupling reactions. *Green Chem.* **2017**, *19* (22), 5488–5493.
 - 36. Yadav, N.; Seidi, F.; Del Gobbo, S.; D’Elia, V.; Crespy, D. Versatile functionalization of polymer nanoparticles with carbonate groups via hydroxyurethane linkages. *Polym. Chem.* **2019**, *10* (26), 3571–3584.
 - 37. Maeda, C.; Shimonishi, J.; Miyazaki, R.; Hasegawa, J.; Ema, T. Highly Active and Robust Metalloporphyrin Catalysts for the Synthesis of Cyclic Carbonates from a Broad Range of Epoxides and Carbon Dioxide. *Chem. Eur. J.* **2016**, *22* (19), 6556–6563.
 - 38. Frisch, M. J.; Trucks, G. W.; Schlegel, H. B.; Scuseria, G. E.; Robb, M. A.; Cheeseman, J. R.; Scalmani, G.; Barone, V.; Mennucci, B.; Petersson, G. A.; Nakatsuji, H.; Caricato, M.; Li, X.; Hratchian, H. P.; Izmaylov, A. F.; Bloino, J.; Zheng, G.; Sonnenberg, J. L.; Hada, M.; Ehara, M.; Toyota, K.; Fukuda, R.; Hasegawa, J.; Ishida, M.; Nakajima, T.; Honda, Y.; Kitao, O.; Nakai, H.; Vreven, T.; Montgomery, J. A.; Peralta, J. E.; Ogliaro, F.; Bearpark, M.; Heyd, J. J.; Brothers, E.; Kudin, K. N.; Staroverov, V. N.; Kobayashi, R.; Normand, J.; Raghavachari, K.; Rendell, A.; Burant, J. C.; Iyengar, S. S.; Tomasi, J.; Cossi, M.; Rega, N.; Millam, J. M.; Klene, M.; Knox, J. E.; Cross, J. B.; Bakken, V.; Adamo, C.; Jaramillo, J.; Gomperts, R.; Stratmann, R. E.; Yazyev, O.; Austin, A. J.; Cammi, R.; Pomelli, C.; Ochterski, J. W.; Martin, R. L.; Morokuma, K.; Zakrzewski, V. G.; Voth, G. A.; Salvador, P.; Dannenberg, J. J.; Dapprich, S.; Daniels, A. D.; Farkas; Foresman, J. B.; Ortiz, J. V.; Cioslowski, J.; Fox, D. J. Gaussian 09. Gaussian 09, Revision B.01. Gaussian Inc.: Wallingford CT 2009.
 - 39. Becke, A. D. Density-functional thermochemistry. III. The role of exact exchange. *J. Chem. Phys.* **1993**, *98*, 5648–5652.
 - 40. Lee, C., Yang, W. & Parr, R. G. Development of the Colle-Salvetti correlation-energy formula into a functional of the electron density. *Phys. Rev. B* **1988**, *37*, 785–789.
 - 41. Peng, C. & Bernhard Schlegel, H. Combining Synchronous Transit and Quasi-Newton Methods to Find Transition States. *Isr. J. Chem.* **1993**, *33*, 449–454.